CONTROL OF DIFFUSIBLE WELD METAL HYDROGEN THROUGH ARC CHEMISTRY MODIFICATIONS

by

JOHN DU PLESSIS

Submitted in partial fulfilment of the requirements for the degree of

MASTER OF SCIENCE (METALLURGY)

in the Faculty of Engineering, the Built Environment and Information Technology

University of Pretoria

Supervisor: Professor M du Toit

May 2006

ABSTRACT

This project examined the feasibility of using flux modification to reduce the as-deposited hydrogen content of basic-type shielded metal arc welds. Additions of oxidizing ingredients (micaceous iron oxides) to the reference flux formulation lowered the diffusible weld hydrogen content by up to 70%. Increasing amounts of silica caused a slight reduction in hydrogen content, probably as a result of the reaction between SiO_2 and CaF_2, which produces SiF_4 and CaO as reaction products. Flux formulations containing additions of fluorine-containing compounds and calcite displayed lower hydrogen levels, with the diffusible weld metal hydrogen content reaching a minimum with increasing additions. Higher levels caused an increase in the weld hydrogen content. Thermodynamic slag modelling attributes the existence of these minima to a decrease in slag water capacity with an increase in slag fluorine content (at constant basicity), brought about by higher concentrations of fluorine-containing compounds in the flux formulation. The effect of flux additions on the weld mechanical properties and the electrode operating characteristics was not evaluated during the course of this investigation.

Key Words

Hydrogen; shielded metal arc welding; basicity; flux; water vapour; oxidizing ingredients; silica; fluorine; calcite; deoxidation.

TABLE OF CONTENTS

CHAPTER 1

INTRODUCTION

1.1 BACKGROUND:

Hydrogen-assisted cold cracking (HACC), also known as *cold cracking*, *delayed cracking* or *underbead cracking*, is one of the most prevalent defects encountered when welding ferritic steels. Hydrogen-induced cracking often occurs some time after welding and, although extensive, may be difficult to detect. It is not confined to welding, but can occur in steels during manufacture, during fabrication and in service.

Hydrogen-assisted cracking has received considerable attention in literature owing to its prevalence [1], and the major variables influencing the incidence of hydrogen-induced cracking in ferritic steels have been defined for many years. Despite extensive research into the phenomenon, it is still experienced regularly by fabricators, particularly when welding high-strength structural steels [2]. A heavy responsibility is placed on the fabricator to incorporate appropriate safeguards against hydrogen cracking in welding procedures. Fabricators generally rely on preheating, interpass temperature control and postweld heat treatment, combined with the use of low-hydrogen basic-type welding consumables (treated in the prescribed manner), to reduce the risk of cracking.

When hydrogen-induced cracking occurs as a result of welding, the cracks may be situated in the heat-affected zone (HAZ) of the base material, or in the weld metal itself. Historically the risk of cracking has been highest in the heat-affected zone (HAZ) of the parent metal, where susceptible microstructures can form as a result of the rapid cooling rates experienced during the weld thermal cycle.

Recent developments in steelmaking and steel processing techniques have resulted in thermo-mechanical controlled process (TMCP) low-carbon and low-alloy steels with reduced carbon equivalents. These steels are less hardenable than higher carbon grades and exhibit improved weldability and lower susceptibility to hydrogen cracking in the HAZ. TMCP steels therefore require less stringent welding procedures (little or no preheat) to prevent HAZ cracking. The development of welding consumables has, however, lagged somewhat behind the development of these preheat-free steels due to the fact that weld deposits consist of as-solidified structures with considerable structural heterogeneity [3]. The increasing use of TMCP steels in welding applications has therefore resulted in a shift in the location of hydrogen-induced cracks from the HAZ into the weld metal.

The traditional methods for controlling hydrogen cracking (preheating, interpass temperature control and postweld heat treatment) are very expensive, both in terms of time and energy. The need for these procedures also negates the advances made in modern steelmaking to

produce the so-called preheat-free steels. An alternative means of controlling hydrogen-induced cracking during welding is to reduce the hydrogen content of the welding consumables. This method is very attractive to welding consumable manufacturers and economical desirable to fabricators.

The development of flux systems with low baseline moisture contents and low moisture pick-up rates has reduced the amount of as-deposited weld metal hydrogen significantly. The potential of these methods for controlling weld metal hydrogen contents has been exploited to the maximum. Welding consumable manufacturers and fabricators worldwide are currently striving to produce welding consumables with increasingly lower as-deposited weld metal hydrogen contents. Current benchmarks are less than 3 ml hydrogen per 100 g of weld metal for basic shielded metal arc welding (SMAW) electrodes, and less than 2 ml hydrogen per 100 g of weld metal for flux cored arc welding (FCAW) consumables.

It has been reported in published literature that the diffusible weld metal hydrogen content can be manipulated through arc chemistry modifications [2, 4-7]. These studies mainly focused on submerged arc wire and flux systems and on flux cored wires. These systems are simplistic in the sense that the flux formulations only contain a limited number of ingredients. Very little has been reported on hydrogen control through arc chemistry modifications in the case of SMAW electrodes.

SMAW is an arc welding process where the heat required for coalescence is supplied by an electric arc that is maintained between the tip of a consumable flux-covered electrode and the workpiece [8]. SMAW electrodes for welding steel typically consist of a mild steel core wire, surrounded by a flux coating that contains numerous mineral, silicate and metal powder ingredients. The flux system is complex to allow for the required electrode operating characteristics and weld metal mechanical properties, as well as ease of manufacture through extrusion.

The Afrox Welding Consumable Factory in Brits, South Africa, produces a range of SMAW consumables. In order to maintain a competitive advantage over imported products, Afrox's range of basic SMAW consumables needs to provide as-deposited weld metal hydrogen contents that compare well with the current international benchmark levels. The objective of this investigation was therefore to examine possible means of lowering the hydrogen potential of the E7018-1 basic-type SMAW electrode presently produced by Afrox. This electrode currently yields an average weld metal hydrogen content of approximately 7 ml per 100 g of weld metal for the range of diameters produced. The project focused on the influence of arc chemistry modifications brought about by variations in flux formulation on the hydrogen content of the deposited weld metal.

The remainder of this chapter describes the mechanism of hydrogen-assisted cold cracking in more detail.

1.2 CONDITIONS LEADING TO HYDROGEN-INDUCED COLD CRACKING IN FERRITIC STEEL WELDS:

As illustrated in Figure 1.1, hydrogen-induced cracking in ferritic steel welds occurs when the following three requirements are satisfied simultaneously [9]:

- sufficient amounts of hydrogen are present in the weld metal,
- tensile stresses act on the weld metal, and
- a crack-sensitive microstructure is present.

The magnitude of each factor and its significance within this three-way relationship have yet to be determined for hydrogen-induced cracking in welds.

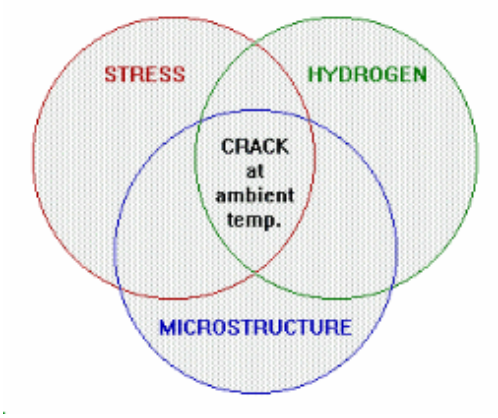

Figure 1.1 The three-way relationship between the three requirements for hydrogen-induced cracking during welding.

It is widely recognised that susceptibility to hydrogen-induced cracking during welding increases with increasing levels of hydrogen, the presence of hard, brittle microstructures in the weld metal or heat-affected zone, and the development of high tensile residual stresses during cooling. Cracking becomes more prevalent as the temperature approaches room temperature. As shown in Figure 1.2, this can be attributed to increases in stress and local hydrogen content with a decrease in temperature.

Each of the requirements for the introduction of hydrogen-induced cracking during welding are briefly considered below.

1.2.1 Hydrogen present in sufficient amounts:

Hydrogen is inevitably present during arc welding and, if present in sufficient amounts, may be absorbed by the weld pool from the arc atmosphere. During cooling, much of this hydrogen escapes from the weld metal through diffusion, but a certain amount also diffuses into the heat-affected zone and the surrounding base metal. The amount of hydrogen that diffuses into the heat-affected zone depends on several factors, including the original amount absorbed, the size of the weld, the

decreasing solubility of hydrogen during cooling, and the cooling rate. In general, the more hydrogen present in the metal, the greater the risk of cracking. Control over the absorbed hydrogen level may be achieved either by minimising the amount initially absorbed, or by ensuring that a sufficient amount of hydrogen is allowed to escape through diffusion before the weld cools. Frequently a combination of both measures provides the best practical solution.

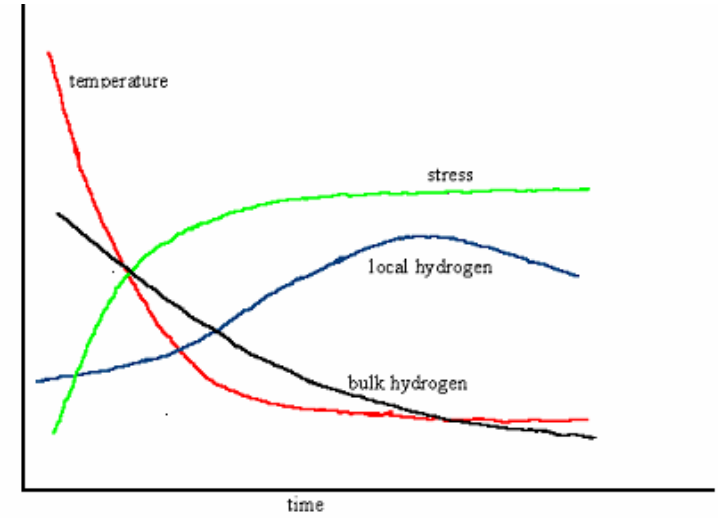

Figure 1.2 Changes in stress, temperature and hydrogen levels as a function of time after completion of the weld [10].

Hydrogen can be introduced into the weld from the base metal being welded, from the welding consumables, or from the surrounding atmosphere [11]. A number of potential hydrogen sources during welding are described below:

- Hydrogen can enter the arc from the base metal, either as hydrogen remaining from the original steelmaking or casting process (particularly in the interior of heavy sections), following service at high temperature and high hydrogen partial pressures, or as a result of corrosion processes, particular sour (i.e. H_2S) service.
- Hydrogen may be present in the consumable core wire as a result of steelmaking and secondary hot working processes.
- Hydrocarbon compounds, such as oil, grease or paint on the plate or core wire surface or adjacent to the weld preparation, can decompose to produce hydrogen in the arc atmosphere. Degreasing fluids used to clean surfaces before welding may likewise decompose to produce hydrogen in the arc.
- Decomposition of hydrated oxides, such as rust on the surface of the base metal or consumable core wire.
- Free moisture in the electrode flux coating.
- Absorbed moisture in the electrode flux coating.

- Crystalline moisture in the flux raw materials.
- Trapped hydroxyl groups in the flux raw materials.
- Moisture pickup from the atmosphere under conditions of high humidity. The diffusible weld metal hydrogen content increases with an increase in the water vapour partial pressure in the ambient atmosphere.

Of these, the major source of weld metal hydrogen during SMAW is moisture present in the electrode flux coating. The flux coating of SMAW electrodes contains numerous ingredients, with varying amounts of crystalline water and absorbed moisture. The absorbed moisture can be released by baking the electrodes at relatively low temperatures (in the region of 110°C to 150°C). The crystalline moisture is, however, more difficult to remove and is normally only released at temperatures of between 400°C to 1000°C [11].

Moisture in the flux coating is also introduced by the silicate binders used to bind the raw material particles in the coating formulation prior to extrusion. The flux coating consists of particles held in a state of agglomeration by the silicate binding material. The resulting porous structure has a large internal surface area to which water molecules can be loosely bound in the form of adsorbed layers. These may range from simple mono-layers, through to multi-layers, and even actual condensation within capillaries.

Hirai *et al* [12] quantified the factors contributing to hydrogen absorption in the weld metal during SMAW. Their model is based upon Sievert's law calculations, and is shown in equation (1.1).

$$H = [\acute{\alpha}^2(\acute{\eta}_1 a_1 + \acute{\eta}_2 a_2) + \beta^2 b]^{1/2} \quad \ldots(1.1)$$

where: H is the absorbed hydrogen content of the weld metal,

a_1 is the as-baked coating moisture content as a weight percentage,

a_2 is the coating moisture absorbed in the time interval between baking and welding (this is defined as the coating moisture content at the time of welding, less the as-baked coating moisture content),

b is the partial pressure of water vapour under ambient atmospheric conditions in mm Hg,

$\acute{\eta}_1$ and $\acute{\eta}_2$ represent the efficiency of moisture transfer from the coating to the arc atmosphere,

$\acute{\alpha}$ is a constant representing the influence of moisture in the coating on the hydrogen content dissolved in the weld metal in ml/100 g $(wt\%)^{1/2}$, and

β is a constant representing the influence of humidity in the ambient atmosphere on the hydrogen content absorbed into the weld metal in ml/100 g $(wt\%)^{1/2}$.

Hirai *et al* concluded that the contribution of chemically combined water in a basic flux coating to the diffusible hydrogen content of the weld metal is significantly higher than that of absorbed moisture. The ambient atmosphere contributes very little hydrogen due to the decomposition of $CaCO_3$ in the arc to form CO_2, and the displacement of moisture-laden air by the protective CO_2 shield. For a basic electrode, the decomposition of $CaCO_3$ results in an arc atmosphere consisting predominantly of carbon monoxide (approximately 77% by volume), carbon dioxide (approximately 19% by volume), with small amounts of hydrogen and water [13].

The chemically bonded moisture, a_1 in equation (1.1), is reduced by the high temperature baking cycle that forms part of the manufacturing process of the electrode. Chew [14] showed that an increase in baking temperature significantly reduces the diffusible hydrogen content of the weld metal. The baking temperature cannot, however, be increased indefinitely to reduce the coating moisture content. At baking temperatures above approximately 480°C, decomposition of the flux constituents starts, which adversely affects shielding gas formation in the arc and the operating characteristics of the electrode during welding.

The absorbed moisture, a_2 in equation (1.1), is a strong function of the humidity of the atmosphere and the exposure time. Hirai *et al* [12] estimated that only 12% of the absorbed moisture in the flux enters the arc atmosphere, compared to 100% of the chemically bonded moisture.

1.2.2 Tensile stresses acting on the weld metal:

Tensile residual stresses inevitably arise from thermal contraction during cooling and may be supplemented by other stresses developed as a result of rigidity in the parts being joined. In rigid structures the natural contraction stresses are intensified because of the restraint imposed on the weld by the different parts of the joint. These stresses concentrate at the toe and root of the weld and also at notches formed by inclusions and other defects.

External stresses applied to a weld soon after completion often supplement these residual stresses and may temporarily increase the risk of cracking. In steel welds, the magnitude of the tensile residual stresses that develop in the weld often approaches the yield stress of the metal [9].

The stress acting upon a weld is a function of the weld size, joint geometry, fit-up, external restraint and the yield strengths of the base metal and weld metal. Hydrogen embrittlement is strain-rate dependent and the risk of cracking is greatest at slow strain rates. As the strain rate is low during the final stages of cooling in the weld, the susceptibility to crack formation is high at this time.

1.2.3 Susceptible microstructure:

The microstructure produced in any steel is essentially dependent upon:

- the cooling rate through the transformation temperature range of the steel in question,
- the composition and the hardenability of the steel, and
- the prior austenite grain size before transformation.

The part of the heat-affected zone that experiences high enough peak temperatures for the base metal to transform to austenite, may harden to form martensite or bainite on cooling as a result of the rapid cooling rates experienced after welding. Hydrogen cracks, when present, are invariably found in these transformed regions. Close to the fusion boundary, the heat-affected zone is raised to a sufficiently high temperature to produce a coarse grain size. This high temperature heat-affected zone, because of its coarse grain structure, is not only more hardenable, but also less ductile than regions further away from the fusion boundary. This is the region where the greatest risk for cracking exists. As a general rule, for both carbon-manganese and low-alloy steels, the harder the microstructure, the greater the risk of hydrogen-induced cracking.

The cooling rate is governed by the heat input during welding, the initial temperature of the parts being joined, as well as the plate thickness and geometry. Control over the cooling rate in a particular fabrication can therefore be achieved by varying heat input and preheat temperature. Preheat and interpass temperature control provides the basis for many welding procedures designed to prevent hydrogen-induced cracking in steel welds.

The hardenability of a steel is governed by its composition, and a useful way of describing hardenability is by assessing the total contribution of all the elements present in the material. The hardenability of a steel base metal can be quantified using empirical carbon equivalent (CE) equations. The carbon equivalent equation shown in equation (1.2), known as the IIW formula, is widely used. Higher CE values usually denote greater hardenability, which points to an increased risk of forming hard, crack-sensitive microstructures like martensite.

$$CE = C + \frac{Mn}{6} + \frac{Cr + Mo + V}{5} + \frac{Ni + Cu}{15} \qquad \ldots(1.2)$$

1.3 THE MECHANISM OF HYDROGEN-INDUCED COLD CRACKING DURING WELDING:

When all three requirements described above are satisfied simultaneously during welding, hydrogen-induced cracks can potentially initiate and propagate through the steel microstructure. Typical locations of these hydrogen-induced cracks in the weld metal and heat-affected zone are illustrated in Figure 1.3.

Whether hydrogen-induced cracks form in the weld metal or in the heat-affected zone depends largely on the stress state and the microstructures that develop in these regions on cooling. If the martensite transformation in

the weld metal occurs at a higher temperature than in the parent metal, the diffusible hydrogen will segregate preferentially to the parent metal heat-affected zone due to the greater hydrogen solubility in austenite. This may result in HAZ underbead cracking. If the martensite start temperature of the parent metal heat-affected zone is higher than that of the weld metal, hydrogen will remain in the weld, increasing the risk of weld metal cracking.

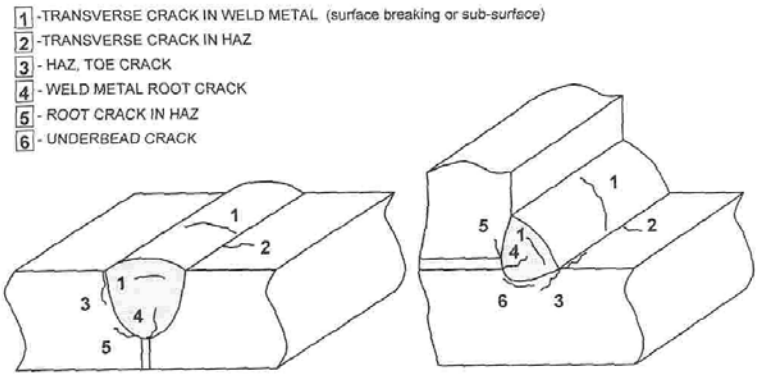

Figure 1.3 Schematic illustration of typical crack locations associated with HACC in welds [15].

This behaviour was described by Olson and Liu [16] for low-alloy steel weldments, as illustrated in equation (1.3).

$$\Delta M_S = \Delta M_{WM} - \Delta M_{HAZ} \quad \ldots(1.3)$$

where : ΔM_S represents the difference between the martensite start temperatures of the weld metal and heat-affected zone (°C),
ΔM_{WM} is the martensite start temperature of the weld metal (°C), and
ΔM_{HAZ} is the martensite start temperature of the parent metal HAZ (°C).

If $\Delta M_S > 0$, hydrogen will accumulate in the parent metal HAZ, and if $\Delta M_S < 0$, hydrogen will accumulate in the weld metal.

Lower weld metal martensite start temperatures extend the temperature range during which the weld is austenitic, and increase the residence time of hydrogen in the weld metal. The temperature range available for hydrogen diffusion to the heat-affected zone is therefore reduced.

Once all the conditions for hydrogen-induced cracking are satisfied, cracks can form in the weld metal or heat-affected zone. Although there is disagreement in the published literature [1,2,17] concerning the exact mechanism of hydrogen-induced cold cracking, the typical sequence of events leading to cracking can be summarised as follows:

- Hydrogen enters the arc atmosphere from the shielding gas, the flux or from surface contamination. The hydrogen is converted to the atomic or ionized state and readily dissolves in the molten weld metal.
- As the weld metal cools, it becomes supersaturated in hydrogen. If the heat-affected zone is still austenitic, the hydrogen diffuses across the fusion line into the austenitized heat-affected zone, which has a higher solubility for hydrogen. If the heat-affected zone transforms before the weld metal, the hydrogen will remain in the weld.
- The hydrogen is retained in the austenite under conditions of rapid cooling. The austenite transforms to crack-sensitive martensite or bainite. The atomic hydrogen is virtually insoluble in the martensitic or bainitic lattice.
- The trapped hydrogen exists in a state of high energy in the lattice. By diffusion it seeks discontinuities in the lattice, where it concentrates.
- The stresses generated by external restraint and by the volume changes due to transformation act with the hydrogen to enlarge the lattice discontinuities to crack size. The hydrogen also accelerates cracking by lowering the cohesive strength of the metal lattice.
- Crack growth carries the crack tip away from the point of hydrogen concentration. Hydrogen then diffuses to the crack tip to facilitate further crack growth.

The 'bulk' hydrogen content in the region of the weld decreases with time as hydrogen diffuses out of the weld metal and the heat-affected zone. At localized highly stressed areas within the weld metal and heat-affected zone, the hydrogen content may, however, remain high for a considerable period of time as a result of stress-assisted diffusion [17].

As described above, the development of hydrogen-induced cracks during welding and the crack location (weld metal or heat-affected zone) depend on the amount of hydrogen absorbed from the arc atmosphere, the solubility of hydrogen in the crystal structure, and on the diffusivity of hydrogen in the steel lattice. These factors are considered in more detail in the following paragraphs.

1.4 THE SOLUBILITY OF HYDROGEN IN STEEL WELDMENTS:

Whether or not hydrogen is available to diffuse to the heat-affected zone during welding to form HAZ cracks, depends to a significant extent on the amount of hydrogen absorbed from the arc atmosphere and the solubility of hydrogen in the weld metal. A number of models describing the hydrogen solubility in liquid metal are considered below.

When a molten metal is exposed to a diatomic gas such as hydrogen (H_2), the equilibrium concentration of the gas in the liquid metal can be determined from Sievert's law. The dissolution reaction of such a diatomic gas, G_2, is shown in equation (1.4). Sievert's law states that the equilibrium gas concentration in the molten metal at a constant temperature is

proportional to the square root of the partial pressure of the diatomic gas above the melt, as shown in equation (1.5).

$$\tfrac{1}{2}G_2\ (g) \rightarrow \underline{G}\ (wt\%) \qquad \ldots(1.4)$$

$$\underline{G}\ (wt\%) = K_{eq}{}^{d}\sqrt{P_{G_2}} = \sqrt{P_{G_2}}\exp\left(-\frac{\Delta G^0}{RT}\right) \qquad \ldots(1.5)$$

where: ΔG^0 is the standard free energy for reaction (1.4),
$\underline{G}$ (wt%) is the dissolved gas concentration in equilibrium with the diatomic gas,
K_{ed} is the equilibrium constant for reaction (1.4),
P_{G_2} is the partial pressure of G_2,
R is the universal gas constant, and
T is the temperature of the liquid metal.

In the absence of an electric arc, the solubility of a diatomic gas such as hydrogen obeys Sievert's law, and this relationship is occasionally extended to the calculation of solubility limits in weld pools. It is often stated in literature that the solubility of diatomic species in the molten weld pool obeys Sievert's law, with the solubility increasing as the partial pressure of the gas in the arc atmosphere increases. Recent research, however, has indicated that the solubility of diatomic gases in arc welds does not follow Sievert's law [18-22].

It has been shown that the solubility of a diatomic gas is significantly higher than the level predicted from equilibrium calculations (Sievert's law) when the liquid metal is in contact with an arc plasma. Calculations based on Sievert's law yield effective reaction temperatures much higher than 2500°C, which was reported by Block-Bolton and Eager [23] as the maximum temperature obtainable in steel arc welds. The solubility increases with increasing gas partial pressure in the arc, until a maximum solubility level is reached. At higher partial pressures, the solubility values remain constant. This maximum solubility limit corresponds to the saturation level of the diatomic gas in the liquid weld metal.

In order to describe the effect of the plasma atmosphere on the hydrogen solubility in liquid weld metal, Gideon and Eager [18] proposed a new model that involves both monatomic and diatomic hydrogen species. This model is based on the premise that the plasma temperature during arc welding is sufficiently high to dissociate diatomic hydrogen molecules, H_2, into monatomic hydrogen, H.

The model assumes that the dissolution of hydrogen in liquid weld metal takes place in two steps:

- the dissociation of diatomic hydrogen in the bulk plasma, and
- the absorption of monatomic hydrogen at the liquid metal interface.

The dissociation of hydrogen molecules in the arc is represented by the following equilibrium reactions:

$$H_2\,(g) \leftrightarrow 2\underline{H} \qquad \ldots(1.6)$$

$$H_2\,(g) \leftrightarrow 2H\,(g) \qquad \ldots(1.7)$$

Equations (1.6) and (1.7) can be combined into a single hydrogen dissolution reaction, described by equation (1.8). The free energy change associated with the dissolution reaction is given by equation (1.9).

$$H(g) \leftrightarrow \underline{H} \qquad \ldots(1.8)$$

$$\Delta G = -44.780 + 3.38T \qquad \ldots(1.9)$$

Since the solubility of monatomic hydrogen in the liquid weld metal is different from that of diatomic hydrogen, Sievert's law cannot be applied in the presence of a plasma phase. Calculations have shown that the amount of absorbed monatomic hydrogen decreases with an increase in weld pool temperature. This implies that the majority of monatomic hydrogen absorption takes place at the cooler edges of the weld pool close to the fusion line. This is in direct contrast to the predictions of Sievert's law which state that maximum absorption occurs in the high temperature region of the weld pool directly under the arc.

The results reported by Gideon and Eager [18] suggest that monatomic hydrogen absorption dominates the overall dissolution of hydrogen from the arc plasma and is responsible for the biggest contribution to the total weld metal hydrogen content. This conclusion was supported by McKeown [11], who proposed that the absorption of hydrogen into the weld pool is dependent on the dissociation of hydrogen gas. The presence of low concentrations of monatomic hydrogen in the arc plasma leads to enhanced solubility over that predicted from Sievert's law calculations. If the hydrogen solubility in the weld metal is exceeded during cooling, hydrogen is available to diffuse from the weld metal into the heat-affected zone, provided the weld metal transforms before the heat-affected zone (as described in §1.3). The diffusion of hydrogen is considered in more detail in §1.6.

Moisture in the arc atmosphere serves as a major source of monatomic hydrogen. The fundamental moisture dissociation reaction during welding is represented by equation (1.10):

$$H_2O_{(g)} = 2[H] + [O] \qquad \ldots(1.10)$$

The amount of oxygen dissolved in the steel has a significant influence on hydrogen absorption from moisture in the arc. Highly deoxidized steel with little oxygen in solution encourages reaction (1.10) to proceed to the right, resulting in the dissolution of more hydrogen in the liquid steel. Low oxygen

weld metal should therefore absorb more hydrogen than a high oxygen weld, given the same moisture content in the arc.

1.5 THE HYDROGEN CONTENT OF THE WELD METAL:

In order to quantify the absorption of hydrogen during welding, it is assumed that the hydrogen concentration in the weld pool at any instant is determined by the difference between the inflow rate of hydrogen and the outflow rate of hydrogen [24].

Inflow of hydrogen is determined by the arc conditions at the interface between the arc and the liquid metal. The arc temperature and the partial pressure of monatomic hydrogen in the arc play a major role, as described in §1.4. Hydrogen can also enter the weld pool due to melting of hydrogen-containing base metal at the leading edge of the pool. Outflow of hydrogen occurs at the surface of the weld pool through the recombination of hydrogen atoms to form H_2, and also through solidification of hydrogen-containing weld metal at the rear of the pool.

The time-dependant change in the hydrogen concentration of the liquid weld metal can therefore be described as [24]:

$$\frac{dH}{dt} = W \frac{dc}{dt}$$

$$= \alpha A - \beta B c + R_m c_o - \eta R_m c \qquad \ldots(1.11)$$

where:
- H is the amount of hydrogen present in the liquid metal,
- t is the time in seconds,
- W is the weight of liquid metal in the weld pool,
- c is the hydrogen concentration in the liquid metal,
- α is the absorption coefficient,
- A is the interfacial area between the arc and liquid metal,
- β is the desorption coefficient,
- B is the interfacial area between the liquid metal and the surrounding atmosphere,
- R_m is the melting rate,
- c_o is the original hydrogen concentration, and
- η is a constant representing the fraction of hydrogen that is frozen in during solidification.

The term αA represents the amount of hydrogen absorbed from the arc. The term $R_m c_o$ represents the amount of hydrogen that enters the weld pool as a result of the melting of hydrogen-containing base material. These two terms represent the total amount of hydrogen entering the weld pool. The hydrogen leaving the weld pool is represented by the loss of hydrogen through solidification, $\eta R_m c$, and hydrogen losses to the atmosphere through the weld pool surface, βBc.

1.6 THE DIFFUSION OF HYDROGEN DURING WELDING:

Once hydrogen has dissolved in the weld pool, this hydrogen can diffuse in two principal directions. During cooling, the hydrogen can escape from the weld through the outer surface by recombining to form H_2, but hydrogen also diffuses to a lesser extent into the heat-affected zone.

Hydrogen is highly mobile in an open metal crystal lattice such as that of steel and diffuses readily during the weld thermal cycle [11]. In its atomic form, hydrogen can pass through the iron (or steel) lattice due to its small size relative to that of the lattice interstices. Hydrogen present in the weld metal can be classified into one of two types, depending on its diffusivity:

- diffusible hydrogen that is dissolved in the weld metal in an atomic or ionic form and is able to diffuse from the weld metal into the atmosphere or heat-affected zone on cooling, and
- residual hydrogen that does not diffuse from the weld metal on cooling.

Under equilibrium conditions in the solid state, steel can exist either as a face centred cubic (FCC) phase known as austenite, or as a body centred cubic (BCC) phase known as α-ferrite. These crystal structures are shown schematically in Figure 1.4.

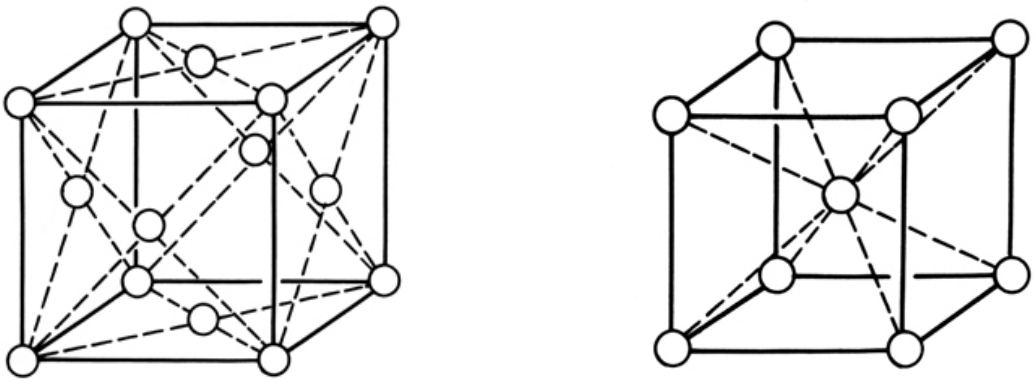

(a) (b)

Figure 1.4 (a) Face centred cubic crystal structure (austenite); and (b) body centred cubic crystal structure (ferrite).

Atomic hydrogen can diffuse more readily through a BCC crystal structure than through an FCC metal structure due to the less densely packed structure of the BCC unit cell. This implies that austenite has a higher solubility for atomic hydrogen than ferrite, brought about by the lower diffusion rate and the slightly larger interstitial openings in the austenite unit cell.

The diffusivity of hydrogen is also a function of temperature, as shown in Figure 1.5. The diffusivity generally decreases with a reduction in temperature, but below approximately 200°C there is an abrupt decrease in the diffusion rate of hydrogen in ferritic steels. This abrupt decrease can be

attributed to the tendency of interstitial atoms to accumulate at lattice imperfections at lower temperatures. This causes hydrogen to be trapped by stationary dislocations in the lattice.

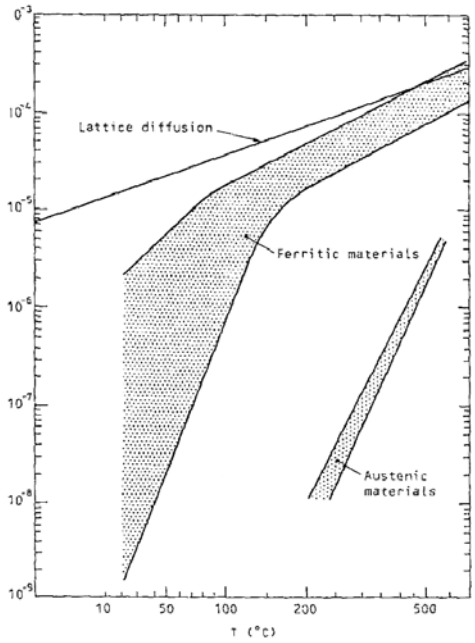

Figure 1.5 The diffusion coefficient of hydrogen as a function of temperature for ferritic and austenitic materials [9].

Various diffusion coefficients for hydrogen in steel and steel weldments have been published in literature. One of the most comprehensive compilations was published in 1995 by Boellinghaus, Hoffmeister and Dangeleit [10]. This summary confirms the existence of a wide range of diffusion coefficients for hydrogen in steel and steel weld metal. The variation in reported hydrogen diffusivities can be attributed to small differences in the microstructure, alloy content, impurity concentration and defect content of the steels evaluated in these investigations.

Some of the factors which affect the diffusion of hydrogen in steel [10] are listed below:

- the presence of internal effects, such as dislocations and crystal lattice defects,
- the incidence of porosity,
- the alloying element content and impurity concentration,
- cold work and applied stress,
- microstructure effects, and
- surface effects.

A summary of the most important factors that influence the hydrogen diffusivity in steel is given in Figure 1.6.

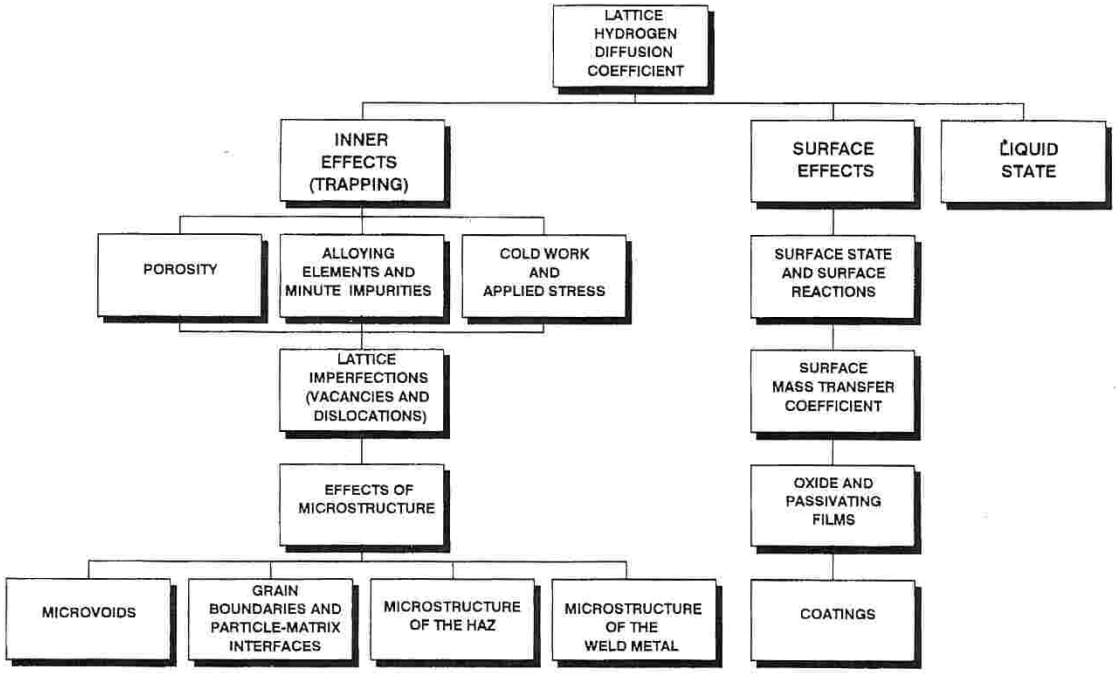

Figure 1.6 Summary of the major factors which influence the hydrogen diffusivity in low carbon mild steels [10].

Grain boundaries normally present accelerated diffusion paths, but no significant difference in hydrogen diffusivity has been reported between fine and coarse grained steels.

The hydrogen diffusion content is also reported to be dependent on the microstructure of martensitic heat-affected zones. Hydrogen diffusion rates increase with an increase in tempering temperature, probably due to the trapping of hydrogen at lattice imperfections produced by the transformation of martensite. The presence of retained austenite in martensite increases the amount of hydrogen trapped at the martensite-austenite interface and therefore reduces hydrogen diffusivity.

Odengard *et al* [25] found that the diffusivity of hydrogen in basic weld metal is a factor of ten higher than that of hydrogen in rutile flux deposits. Hydrogen diffusivity in rutile weld metal is apparently retarded by the presence of more non-metallic slag inclusions and oxygen in the lattice. Hydrogen evolution from steel is also delayed by the existence of micro-voids at the interface between the steel lattice and manganese sulphide inclusions.

The presence of an oxide film on the steel surface also tends to reduce hydrogen diffusivity by acting as a diffusion barrier between the atmosphere and the underlying weld metal. This inhibits the recombination of hydrogen atoms to form H_2 at the weld surface.

1.7 THE WATER VAPOUR SOLUBILITY OF SLAG:

The solubility of water vapour in molten slag, i.e. the hydroxyl capacity, C_{OH}, provides important information for controlling the hydrogen content of molten steel [26]. Hydrogen pick-up in the weld pool is strongly dependent on the water vapour solubility in the slag. The concentrations of both hydrogen and oxygen in the weld pool are expected to be proportional to the concentration of hydroxyl ions in the slag.

Ban-ya and co-workers [26] reported that the activity coefficient of a component in a multi-component slag can be described by a quadratic formalism based on the regular solution model. The activity coefficient of component *i* in a multi-component regular solution can therefore be expressed as:

$$G_i = \Delta H_i = RT \ln \gamma_i$$
$$= \Sigma_j \alpha_{ij} X^2_j + \Sigma_j \Sigma_k (\alpha_{ij} + \alpha_{ik} - \alpha_{jk}) X_j X_k \quad \ldots(1.12)$$

where: X_i is the cation fraction, and
α_{ij} is the interaction energy between cations.

The hydroxyl capacity can be estimated from the regular solution (RS) model in the following way:

$$\tfrac{1}{2} H_2O = HO_{0.5} \text{ (RS)} \quad \ldots(1.13)$$

$$RT \ln K_{H_2O} = RT \ln X_{HO_{0.5}} - \tfrac{1}{2} \log P_{H_2O} + RT \ln \gamma_{HO_{0.5}} \text{ (RS)} \quad \ldots(1.14)$$

The hydroxyl capacity can therefore be expressed as:

$$RT \ln C_{OH} = RT \ln K_{H_2O} - \Sigma_i \alpha_{H\text{-}i} X^2_i - \Sigma_i \Sigma_j (\alpha_{H\text{-}I} + \alpha_{H\text{-}j} - \alpha_{ij}) X_i X_j \quad \ldots(1.15)$$

It is therefore possible to calculate the hydroxyl capacity of any slag composition as a function of temperature.

It has been shown that the water vapour solubility in slag is proportional to the square root of the water vapour pressure in the gas phase and that the hydroxyl capacity is only a function of temperature and the slag composition. The hydroxyl capacity, C_{OH}, is given by equation (1.16):

$$C_{OH} = \frac{\%H_2O}{\sqrt{\frac{P_{H_2O}}{P^0}}} \quad \ldots(1.16)$$

where: $\%H_2O$ is the weight percentage water in the slag,
P_{H_2O} is the partial pressure of water vapour in the gas phase in equilibrium with the molten slag, and
P^0 is atmospheric pressure.

The molar hydroxyl capacity is defined as:

$$C'_{OH} = \frac{X_{HO_{0.5}}}{\sqrt{\frac{P_{H_2O}}{P^0}}} \qquad ...(1.17)$$

where: $X_{HO_{0.5}}$ is the mole fraction of $HO_{0.5}$ in the molten slag.

Ban-ya *et al* [26] reported that the hydroxyl capacity decreases with an increase in basicity, but reaches a distinct minimum value at approximately unit basicity. At higher slag basicity levels, the hydroxyl capacity tends to increase.

The dependence of the hydroxyl capacity on slag composition can be explained by a change in the state of water vapour dissolved in the slag with changes in the slag basicity. Water vapour dissolves in molten slag in accordance with the following reactions, where (O^0), (O^-) and (O^{2-}) represent bridging, non-bridging and free oxygen ions, respectively, (OH) is the hydroxide and (OH^-) the hydroxyl ion in the slag.

Acidic slag $(O^0) + H_2O(g) = 2(OH)$ ...(1.18)

Basic slag $2(O^-) + H_2O(g) = (O^{2-}) + 2(OH)$ ...(1.19)

$2(O^-) + H_2O(g) = (O^0) + 2(OH^-)$ ...(1.20)

Equation (1.18) represents the breakdown of silicate networks by hydroxyl ions in acidic slags. Water acts as a chain breaker in these slags.

Equations (1.19) and (1.20) represent the reaction of water vapour with free oxygen ions in basic slags. Water acts as a chain former in these slags. The water vapour in the gaseous phase above the liquid slag reacts with free oxygen ions. The slag then transfers the hydrogen in the form of hydroxyl ions to the liquid weld pool.

In a slag of neutral basicity, neither of the mechanisms described in equations (1.18) to (1.20) are favoured, and the solubility of water vapour in the slag is minimized.

As described above, the hydroxyl capacity of a slag is directly related to the oxygen activity in the slag [27]. Figure 1.7 shows the relationship between the hydroxyl capacity and the composition of three alkali silicates [26]. It is evident that a minimum water capacity is reached in each of the three alkali silicate slags. The existence of this minimum value is attributed to the amphoteric behaviour of water in slag systems.

The water vapour solubility of slags will be revisited in §5.4.2 as a means of explaining some of the experimental results obtained during the course of this investigation. These experimental results focus on the diffusible

weld metal hydrogen contents measured in shielded metal arc welds deposited using electrodes with a range of experimental flux coatings. These consumables were designed in order to evaluate the effectiveness of various theoretical hydrogen reduction strategies based on arc chemistry modification. These hydrogen reduction models are considered in more detail in Chapter 2.

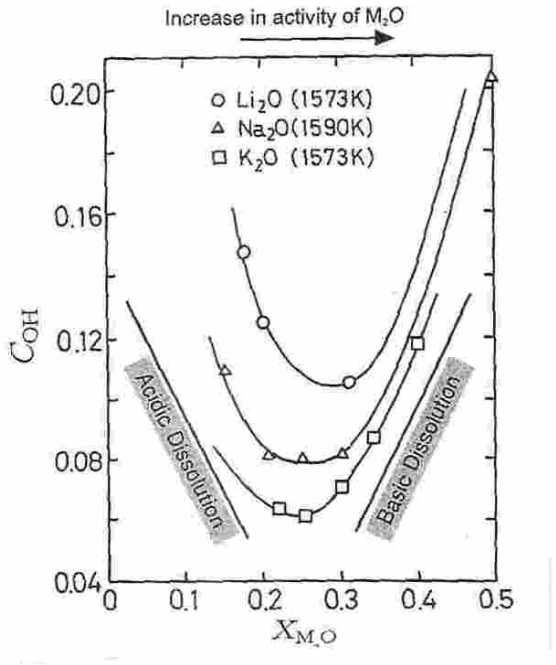

Figure 1.7 The relationship between the hydroxyl capacity and the composition of alkali silicates [26].

CHAPTER 2

STRATEGIES FOR REDUCING THE DIFFUSIBLE WELD METAL HYDROGEN CONTENT

A number of theoretical models have been proposed in published literature as means of reducing weld metal hydrogen contents [2,4-6,28]. Some of these hydrogen reduction models are briefly summarized below:

- Reducing the amount of hydrogen entering the weld pool by modifying the chemistry of the arc plasma through additions of oxidizing ingredients and fluoride-containing compounds to the flux formulation.
- Trapping hydrogen in the metal lattice, for example at dislocations, grain boundaries or carbides particles.
- Increasing the slag basicity to reduce the diffusible hydrogen content of the weld metal.
- Decreasing the partial pressure of hydrogen in the arc to reduce the amount of hydrogen absorbed by the weld metal.
- Adding ingredients to the flux formulation that react with hydrogen to form insoluble hydrogen-containing products in the liquid iron.
- Trapping the hydrogen in the solidified steel weld metal.

Some of these theoretical models suggest means of reducing the diffusible hydrogen content of shielded metal arc welds through modification of the electrode coating formulation. A brief overview of the relevant hydrogen reduction strategies is presented in the remainder of this chapter.

2.1 REDUCING WELD METAL HYDROGEN CONTENTS THROUGH THE ADDITION OF OXIDIZING INGREDIENTS TO THE ELECTRODE FLUX FORMULATION:

Oxygen can be introduced into the arc atmosphere through the decomposition of oxidizing ingredients added to the flux formulation. The influence of oxygen on hydrogen absorption during welding can be explained on the basis of the decomposition of moisture in the arc atmosphere, as represented by equation (2.1).

$$H_2O_{(g)} \leftrightarrow 2H + O \qquad \ldots(2.1)$$

According to Le Chatelier's principle, an increase in the oxygen content of the arc atmosphere during welding should encourage equation (2.1) to proceed to the left. This removes monatomic hydrogen from the arc atmosphere, effectively reducing the partial pressure of hydrogen in contact with the liquid weld metal. At the low hydrogen levels normally present in the arc atmosphere during shielded metal arc welding with basic electrodes, Sievert's law predicts a corresponding decrease in the

absorbed hydrogen content of the weld metal. Increasing the oxygen level in the arc is therefore expected to lead to a reduction in the weld metal hydrogen content.

One potential drawback of this method is that the weld may contain higher oxygen levels after welding, which may have a detrimental effect on the weld metal mechanical properties. High levels of oxygen in the weld metal can also result in excessive losses of deoxidising elements (such as manganese and silicon) to the slag. Depletion of manganese and silicon from the weld metal may also have a negative impact on mechanical properties.

2.2 INCREASING THE SLAG BASICITY TO REDUCE THE HYDROGEN CONTENT IN THE WELD METAL:

The concept of slag basicity was first adopted in response to the needs of the steel industry, where basicity is used to evaluate the sulphur-refinement ability of slags in steel ladle refining practices. The use of the basicity index has subsequently been expanded to approximate the oxidation capacity of fluxes, and these principles are now widely applied to characterize the physical and chemical properties of flux systems for welding [29].

Basicity is related to the ease with which oxides dissociate into cations and oxygen anions [29]. Oxides that dissociate readily are termed 'basic' and those that only partially dissociate are termed 'acidic'. A high basicity slag is therefore considered to have a high concentration or high activity of free oxygen ions, O^{2-}.

The basicity index of flux is usually calculated by dividing the total weight percentage of basic flux components by the sum of the acidic and amphoteric components, as shown in equation (2.2)

$$\text{Basicity} = \frac{\sum \text{Basic oxides}}{\sum \text{Acidic and amphoteric oxides}} \qquad \ldots(2.2)$$

Numerous basicity indices for fluxes have been derived to date. The most commonly used empirical basicity index was developed by Tuliani *et al* [30], and is shown in equation (2.3).

$$B = \frac{CaO + MgO + BaO + K_2O + Li_2O + CaF_2 + 0.5(MnO + FeO)}{SiO_2 + 0.5(Al_2O_3 + TiO_2 + ZrO_2)} \qquad \ldots(2.3)$$

Each basic or acidic ingredient in equation (2.3) is represented by its weight percentage in the flux formulation. According to the International Institute of Welding, a flux is termed acidic when the basicity index is less than 1, neutral when it is between 1 and 1.5, semi-basic when it is between 1.5 and 2.5, and basic when the basicity index is greater than 2.5.

In welding, the slag basicity has been shown to correlate the weld metal chemical composition, specifically the oxygen and sulphur contents, to the chemical composition of the slag. In general, weld metal oxygen levels decrease with an increase in the flux basicity [31]. This in turn influences the partitioning of deoxidising elements, in particular manganese and silicon, between the weld metal and the slag.

The basicity index of a flux also has a significant influence on the weld metal hydrogen content. Terashima *et al* [32] reported a reduction in the diffusible hydrogen levels in welds investigated by these authors from 12 to 2 ml/100 g of weld metal when the basicity index was increased from 0 to 3. Chew [33] demonstrated a considerable reduction in the weld metal hydrogen level with an increase in the coating $CaCO_3$ content, as shown in Figure 2.1. This reduction in hydrogen level can be attributed in part to an increase in slag basicity, since $CaCO_3$ decomposes to form CaO (a basic oxide) during welding. Dissociation of $CaCO_3$, however, also introduces oxygen into the arc atmosphere. The higher levels of oxygen in the arc are expected to contribute to the observed lower hydrogen levels (as described in §2.1).

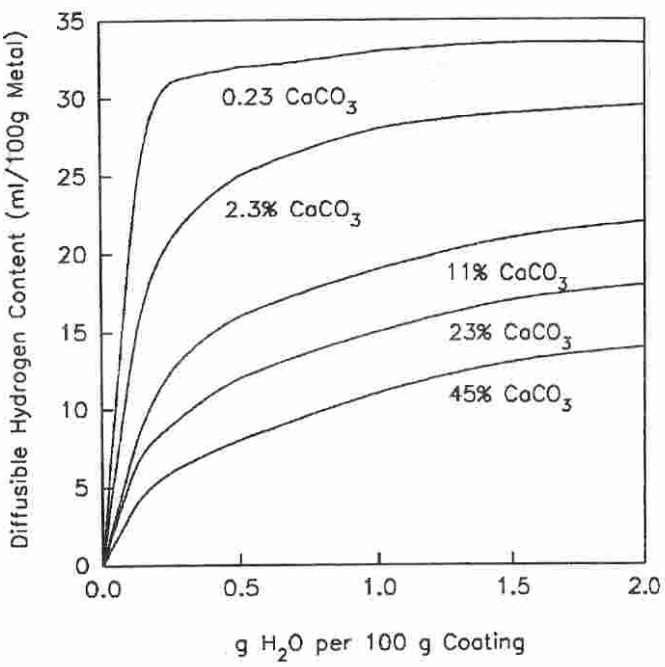

Figure 2.1 The effect of $CaCO_3$ in the electrode coating on the weld metal diffusible hydrogen content [33].

It must be emphasized that the flux basicity of SMAW electrodes cannot be arbitrarily changed, as the various flux ingredients also influence the weld metal composition, mechanical properties, arc stability, arc force, weld pool viscosity, weld bead shape and welding characteristics. The SMAW consumable manufacturer has to find a balance between the operational characteristics of the electrode and the as-deposited weld metal chemical, physical and mechanical properties. In order to optimise one property, another characteristic often has to be compromised.

The basicity of a flux can also be represented by the optical basicity, Λ. Sommerville [34] has shown that the average value of the optical basicity can be calculated from equation (2.4) for any slag composition, where X is the equivalent cation fraction of each oxide in the flux formulation, and Λ_{AOX} and Λ_{BOX} represent the contributions of each oxide in the slag to the average optical basicity.

$$\Lambda = X_{AOX}\Lambda_{AOX} + X_{BOX}\Lambda_{BOX} + \ldots \quad \ldots(2.4)$$

An alternative expression for the optical basicity, given in equation (2.5) was developed by Baune [29]. In this equation Z_c is the coordination number of the cation, R_c is the ratio of the number of moles of the cation over the total number of moles of oxygen in the flux system, and X_c is the Pauling cation electronegativity.

$$\Lambda = \Sigma_{Cations}\,[(Z_c x R_{c)} / (2.78(X_c - 0.26))] \quad \ldots(2.5)$$

Excellent correlation between the optical basicity and the water capacity of slag has been reported. It has been shown that the water capacity can be expressed as a function of the optical basicity, as demonstrated by equation (2.6).

$$\log C_{H_2O} = 12.04 - 32.63\Lambda + 32.71\Lambda^2 - 6.62\Lambda^3 \quad \ldots(2.6)$$

In many slag systems a minimum in water vapour solubility has been observed near neutral basicity.

2.3 DECREASING THE PARTIAL PRESSURE OF HYDROGEN IN THE ARC ATMOSPHERE:

Although the presence of monatomic hydrogen, ionized hydrogen species and excited hydrogen molecules, ions and atoms in the arc plasma implies that Sievert's law is not valid under arc welding conditions, published results (considered in more detail in §1.4) indicate that the weld metal hydrogen content increases linearly with the square root of the partial pressure of hydrogen at low hydrogen partial pressures in the arc. Decreasing the partial pressure of hydrogen in the arc atmosphere should therefore reduce the amount of hydrogen absorbed by the weld metal.

2.4 REDUCING WELD METAL HYDROGEN CONTENTS THROUGH THE ADDITION OF FLUORIDE-CONTAINING INGREDIENTS TO THE FLUX FORMULATION:

Fluorine added to the flux coating is reported to react with hydrogen to form reaction products that are insoluble in liquid iron [4]. As shown in equation (2.7), an increase in fluorine content drives the reaction to the right, reducing the diffusible weld metal hydrogen content.

$$F_2 + H_2 \leftrightarrow 2HF \quad \ldots(2.7)$$

Fluorspar (CaF_2) is widely used as a flux constituent in basic-type electrodes. The fluorine in fluorspar reacts with hydrogen to form insoluble products, as demonstrated by equation (2.7). In the presence of silica, fluorspar also reacts with SiO_2 in the flux to form SiF_4, which functions as a shielding gas and reduces the partial pressure of hydrogen in the arc plasma [35]. This reaction is represented by equation (2.8). The CaO formed as a product of the reaction is expected to increase the basicity index of the slag. All these mechanisms act together to reduce the diffusible weld metal hydrogen level.

$$2CaF_2 + SiO_2 \rightarrow SiF_4 + 2CaO \quad \ldots(2.8)$$

The decomposition of CaF_2 during welding is, however, not particularly active and a significant fraction of the CaF_2 remains in the slag. Researchers have therefore been examining alternative fluoride-containing compounds in order to identify flux additions which may be more effective in reducing weld metal hydrogen levels than CaF_2. Some of the complex fluoride-containing compounds that may be considered as alternatives are Na_3AlF_6, Na_2SiF_6, Na_2TiF_6, K_2SiF_6, K_2AlF_6 and K_2TiF_6.

In order to model the reactions that occur in the welding arc and slag during welding in the presence of CaF_2-containing flux [36], several assumptions need to be made. These assumptions include:

- The reactions occur at rates sufficiently fast to reach equilibrium.
- Liquids and gases in the system act as ideal solutions. The activities of the elements can therefore be expressed as their atomic fractions in the liquid or the gas state.
- The arc is a closed system, i.e. there is no exchange of elements.

In the presence of CaF_2 in the flux, the following reaction is assumed to occur on the surface of the slag:

$$CaF_2\,(slag) + H_2\,(gas) = Ca\,(slag) + 2HF\,(gas) \quad \ldots(2.9)$$

This reaction can be viewed as the combined reaction of the decomposition of CaF_2 (equation (2.10)) and the generation of HF in the presence of hydrogen (equation (2.11)).

$$CaF_2 = Ca + F_2 \quad \ldots(2.10)$$

$$H_2 + F_2 = 2HF \quad \ldots(2.11)$$

The molar free energies of these reactions can be expressed as:

$$\Delta G_{CaF_2} = \Delta G^0_{CaF_2} + RT \ln K_{CaF_2} \quad \ldots(2.12)$$

$$\Delta G_{HF} = \Delta G^0_{HF} + RT \ln K_{HF} \quad \ldots(2.13)$$

where $\Delta G^0_{CaF_2}$ and ΔG^0_{HF} are the standard free energies of reactions (2.10) and (2.11), respectively, *T* is the temperature, *R* is the universal gas constant, and K_{CaF_2} and K_{HF} are the equilibrium constants for reactions (2.10) and (2.11).

The equilibrium constants can be expressed as:

$$K_{CaF_2} = \frac{a_{Ca}\, a_{F_2}}{a_{CaF_2}} \qquad \ldots(2.14)$$

$$K_{HF} = \frac{a_{HF}}{(a_{H_2})^{0.5}(a_{F_2})^{0.5}} \qquad \ldots(2.15)$$

At equilibrium, $\Delta G = 0$, and equations (2.12) and (2.13) become:

$$\Delta G^0_{CaF_2} = -RT \ln K_{CaF_2} \qquad \ldots(2.16)$$

$$\Delta G^0_{HF} = -RT \ln K_{HF} \qquad \ldots(2.17)$$

The free energy of the initial reaction at the slag surface can therefore be expressed by a combination of the free energy equations representing the decomposition of CaF_2 and the generation of HF, as shown in equation (2.18).

$$\begin{aligned} \Delta G^0_{CaF_2} + 2\Delta G^0_{HF} &= -RT \ln K_{CaF_2} - 2RT \ln K_{HF} \\ &= -RT \ln K_{CaF_2}.K_{HF}^{\,2} \end{aligned} \qquad \ldots(2.18)$$

Substituting equations (2.14) and (2.15), equation (2.18) becomes:

$$\begin{aligned} K_{CaF_2}.K_{HF}^{\,2} &= \frac{a_{Ca}\, a_{HF}^{\,2}}{a_{CaF_2}\, a_{H_2}} \\ &= \exp\left[(-\Delta G^0_{CaF_2} + 2\Delta G^0_{HF})/RT\right] \end{aligned} \qquad \ldots(2.19)$$

Assuming that the slag and gas are ideal solutions, the activities of the components in equation (2.19) can be substituted with the molar fractions of the components in the slag or gas.

2.5 FINAL COMMENTS:

It must be emphasized that, although each of these theoretical hydrogen reduction models were described separately, they are all interdependent. For example, a change in the oxidizing content of the flux formulation may also influence the basicity, whereas a change in basicity can vary the hydrogen partial pressure in the arc. In practice, many or all of these mechanisms act together to determine the diffusible hydrogen content of the weld metal. Depending on the composition of the weld metal and the

slag, a particular mechanism may dominate at any particular stage during the weld thermal cycle.

This complicates any attempt to investigate the influence of these mechanisms on the weld metal hydrogen content in isolation. Although the roles played by the different models in controlling the weld metal hydrogen content cannot be separated effectively, Chapter 4 will describe the experimental procedure followed during the course of this investigation in an attempt to quantify the effect of each mechanism on the weld metal hydrogen content.

CHAPTER 3

OBJECTIVES OF THE INVESTIGATION

This project aimed at examining whether changes in arc chemistry, brought about by variations in the composition of the electrode coating, can influence the diffusible hydrogen content of welds. The flux formulations evaluated during the course of this investigation were designed on the basis of the hydrogen reduction models described in the previous chapter, using the standard flux formulation of a basic-type E7018-1 SMAW electrode as reference. The influence of the following flux ingredients on the diffusible weld metal hydrogen content was evaluated:

- the addition of oxidizing ingredients in the form of micaceous iron oxide,
- the addition of silica, SiO_2, as a means of varying the basicity of the flux,
- the addition of various fluoride-containing ingredients, including CaF_2, NaF and two complex fluoride-containing compounds: K_2TiF_6 and K_2AlF_6, and
- the addition of calcite, $CaCO_3$.

The investigation focused on the influence of flux chemistry on the diffusible hydrogen content. The effect of variations in flux composition on the operating characteristics of the electrodes or the properties of the weld metal was not evaluated.

CHAPTER 4

EXPERIMENTAL PROCEDURE

During the course of this investigation, the theoretical models described in Chapter 2 for lowering the diffusible weld metal hydrogen content through arc chemistry modification were examined. The experimental procedure designed to evaluate these models is described below.

4.1 EXPERIMENTAL ELECTRODE PRODUCTION:

During the course of this investigation, a series of experimental electrodes with different flux formulations was produced. The experimental electrodes were produced in small batches (1 kg flux each) in the development laboratory at the Afrox Welding Consumable Factory in Brits, South Africa. The raw materials used to produce the flux mixtures were typical of the ingredients used in the normal day-to-day production of electrodes in the factory.

As a reference, the coating composition of an E7018-1 basic-type welding electrode was selected. This base flux formulation contains up to 16 different ingredients, constituting a very complex system. The coating contains the following major compounds:

- Fluorspar (CaF_2) 22%
- Calcite ($CaCO_3$) and dolomite ($CaCO_3.MgCO_3$) 20%
- Iron powder 31%
- Slag formers, binders, extrusion aids and deoxidizers 27%

(These percentages are approximations only).

The raw materials were weighed and combined in a small blade mixer. Raw materials from the same batches were used throughout the investigation. The dry raw materials were mixed for approximately 7 minutes to obtain a homogeneous dry flux mixture. A liquid silicate binder was then added to the dry flux mixture, followed by mixing for a further 10 minutes. The binder consists of a complex mixture of different alkali silicates with a wide range of viscosities. The flux was then extruded onto a 4 mm diameter mild steel core wire using a coating factor of 1.67, where the coating factor represents the ratio of the core wire diameter to the final electrode diameter. Core wire from the same cast was used for all the experimental electrodes.

After extrusion the electrodes were baked in accordance with the prescribed cycle for an E7018-1 type electrode. The baking cycle consisted of 2 hours at 180°C, followed by a further 2 hours at 460°C. These baking cycles are less complex than those used in the production of large batches of electrodes in the factory.

4.2 EXPERIMENTAL FLUX FORMULATIONS:

The experimental flux formulations evaluated during the course of this project were designed to examine the influence of oxidizing ingredients, flux basicity, various fluoride-containing compounds and calcite flux additions on the diffusible weld metal hydrogen content. The flux formulations investigated are described below.

4.2.1 The influence of oxidizing ingredients in the flux formulation on the diffusible weld metal hydrogen content:

In the first series of experiments, the level of oxidizing ingredients in the electrode flux was modified. As described in Chapter 2, increasing the oxygen content of the arc atmosphere reduces the hydrogen partial pressure in the arc, which should decrease the amount of hydrogen absorbed by the weld metal. In order to evaluate this mechanism, micaceous iron oxide was added to the standard flux formulation in order to increase the amount of oxygen available in the arc.

Micaceous iron oxide (MIO) is a naturally occurring mineral ore, also known as specular hematite. The micaceous iron oxide used as raw material in this part of the investigation contained a minimum of 90% Fe_2O_3 and a maximum of 4% SiO_2.

In the first experimental fluxes produced during this part of the investigation, the micaceous iron oxide was added to the standard flux formulation without varying any of the other ingredients. This resulted in progressive dilution of the other flux ingredients with increasing MIO content. The following flux formulations were produced:

- No MIO addition (the reference electrode formulation),
- addition of 2.4% MIO,
- addition of 4.7% MIO,
- addition of 8.9% MIO, and
- addition of 16.3% MIO.

In the second series of MIO-containing fluxes, the iron powder in the reference formulation was progressively substituted with micaceous iron oxide. The sum total of the weight percentages of MIO and iron powder in the coating therefore remained constant at about 31% (the reference flux iron powder content). The substitutions were done in the following way:

- No substitution (the reference electrode formulation),
- 2.4% MIO,
- 4.9% MIO,
- 9.8% MIO,
- 19.5% MIO, and
- 31.2% (total substitution of iron powder with MIO).

4.2.2 Varying the flux basicity by increasing the SiO_2 content of the flux formulation:

In the second series of experiments, the amount of silica (SiO_2) in the flux formulation was varied in order to change the basicity of the flux. Additions of silica decrease the basicity of the flux as measured by the IIW basicity index given in equation (4.1). The flux therefore becomes more 'acidic' with an increase in SiO_2 content. Increasing flux basicity is expected to decrease the diffusible weld metal hydrogen content.

$$B = \frac{CaO + MgO + BaO + K_2O + Li_2O + CaF_2 + 0.5(MnO + FeO)}{SiO_2 + 0.5(Al_2O_3 + TiO_2 + ZrO_2)} \quad \ldots(4.1)$$

In order to determine the influence of flux basicity on the weld metal hydrogen content, the amount of silica in the flux formulation was varied from 1.3% to 13.1% by weight.

4.2.3 The influence of various fluoride-containing compounds on the weld metal hydrogen content:

In the third series of experiments, the influence of various fluoride-containing flux compounds on the weld metal hydrogen content was investigated. The experimental flux formulations are described below:

- The amount of fluorspar (CaF_2) in the flux coating was varied from 0% to 34% by weight.
- Sodium fluoride (NaF) was added to the reference flux coating in amounts ranging from 0% to approximately 8.9% by weight.
- The fluorspar in the flux coating was progressively substituted with NaF, keeping the sum total of CaF_2 and NaF at a constant level of approximately 21.6% by weight. The following CaF_2 and NaF contents were examined:

  $\rightarrow$21.6% CaF_2 and 0% NaF (the reference flux formulation),
  $\rightarrow$17.4% CaF_2 and 4.3% NaF,
  $\rightarrow$13.1% CaF_2 and 8.6% NaF,
  $\rightarrow$11.7% CaF_2 and 11.7% NaF,
  $\rightarrow$8.6% CaF_2 and 13.1% NaF, and
  $\rightarrow$0% CaF_2 and 21.6% NaF (complete substitution).
- The influence of complex fluoride-containing compounds on the weld metal hydrogen content was evaluated by adding K_2TiF_6 and K_2AlF_6 to the reference flux formulation. K_2TiF_6 was added in amounts of 2.1% or 4.7%. K_2AlF_6 was added to the base flux formulation in amounts of 4.7% or 8.9%.

4.2.4 The influence of calcite additions to the flux on the weld metal hydrogen content:

In the fourth series of experiments, the influence of variations in the calcite ($CaCO_3$) content of the flux on the weld metal hydrogen content was investigated. The percentage calcite in the flux formulation was varied from 10% to almost 24% (the reference formulation contains approximately 16% calcite).

4.3 DETERMINATION OF THE DIFFUSIBLE WELD METAL HYDROGEN CONTENTS:

The hydrogen content of each weld was determined using the standard laboratory method applied at the welding consumable factory. This method is based on the procedure described in ISO 3690: "Procedure for determining the hydrogen content in arc weld metal", but a Yanaco G-1006H gas chromatograph was used to measure the diffusible weld metal hydrogen, instead of the more traditional mercury method. An investigation by an American Welding Society task group indicated that the reproducibility and reliability of this test method is ± 1ml / 100 g weld metal. Similar levels of reproducibility and reliability have been reported by an Australian study [37].

ISO 3690 specifies the sampling and analytical procedure for the determination of diffusible and residual hydrogen in ferritic weld metal. The test consists of a single weld bead deposited under controlled conditions. This weld is rapidly quenched after welding and stored at -78°C or lower until analysed. The copper jig shown in Figure 4.1 was used to ensure uniform clamping and heat dissipation during the test. In order to ensure repeatability, the same welder was used to produce all the experimental welds in this investigation. The welding parameters were maintained at 185 A (15 A less than the maximum recommended by the manufacturer) and 23 V.

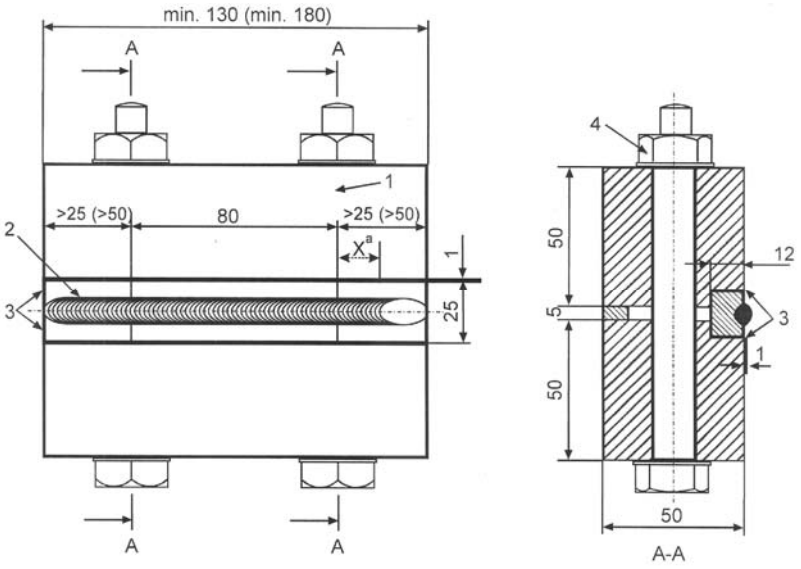

Figure 4.1 Jig used for hydrogen testing in accordance with ISO 3690.

After measuring the amount of weld metal hydrogen, the values were corrected for standard temperature, atmospheric pressure and humidity conditions.

CHAPTER 5

RESULTS AND DISCUSSION

This chapter presents the results of diffusible weld metal hydrogen measurements of welds produced using the experimental electrode flux formulations described in the previous chapter. An attempt is also made to explain some of the trends observed from the extent of partitioning of elements between the weld metal and the slag during welding.

5.1 THE EFFECTS OF OXIDIZING FLUX INGREDIENTS ON THE DIFFUSIBLE WELD METAL HYDROGEN CONTENT:

In the first series of experiments, the influence of oxidizing ingredients in the flux on the diffusible hydrogen content of the weld metal was evaluated by adding micaceous iron oxide (MIO) to the flux formulation. This was done by adding MIO to the base electrode flux formulation in the first set of experiments, and by progressively substituting the iron powder in the base formulation with MIO in the second set of experiments. The diffusible weld metal hydrogen contents measured in these welds are shown in Figure 5.1. Each data point shown in Figure 5.1 indicates the average of eight hydrogen measurements, whereas the error bars represent the range from the minimum to the maximum hydrogen level measured in each formulation.

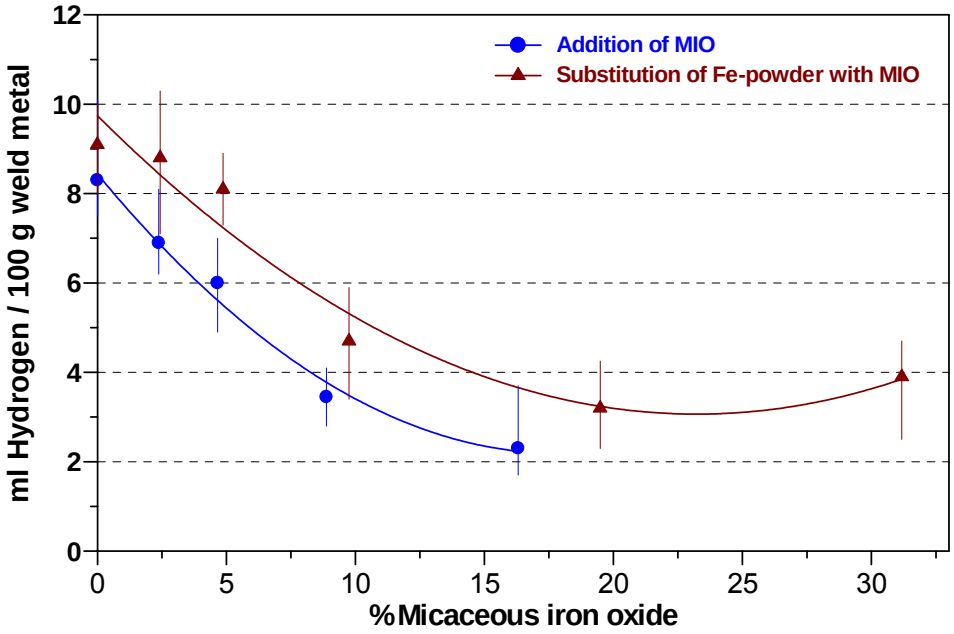

Figure 5.1 Diffusible weld metal hydrogen contents measured as a function of micaceous iron oxide content for flux formulations containing an addition of MIO, and for flux where the iron powder in the base formulation was progressively substituted with MIO.

The addition of MIO to the flux formulation resulted in a significant reduction in weld metal hydrogen content. The presence of 16.3% MIO in the flux coating reduced the weld metal hydrogen content by almost 70%,

compared to the hydrogen level measured in a flux without MIO. The primary mechanism responsible for the reduction in weld metal hydrogen content can be explained by considering the chemical reactions that take place in the weld pool and the arc during welding.

The micaceous iron oxide (MIO) decomposes in the arc during welding to form FeO. The FeO reacts with hydrogen, as described by the reaction shown in equation (5.1), reducing the weld metal hydrogen content.

$$FeO + 2H \leftrightarrow Fe + H_2O_{(g)} \quad \ldots(5.1)$$

At the same time, the partial pressure of hydrogen in the arc is reduced due to dilution of the arc atmosphere with oxygen liberated on dissociation of the H_2O formed as a product of reaction (5.1). This dissociation reaction is represented by equation (5.2). According to Le Chatelier's principle, any increase in the dissolved oxygen content of the weld metal drives reaction (5.2) to the left, removing hydrogen from solution. In equation (5.2), H_2O is in the gaseous state, while $\underline{O}$ and $\underline{H}$ denote oxygen and hydrogen dissolved in the liquid steel.

$$H_2O_{(g)} \leftrightarrow 2\underline{H} + \underline{O} \quad \ldots(5.2)$$

The standard free energy, $\Delta G°$, of the moisture dissociation reaction is given by equation (5.3), where *T* is the temperature [28].

$$\Delta G° = 46.18 + 1.57T \quad \ldots(5.3)$$

The equilibrium constant, K_1, for this reaction can be expressed as:

$$K_1 = \frac{[\underline{H}]^2[\underline{O}]}{P_{H_2O}} \quad \ldots(5.4)$$

If the dissolved hydrogen content, [$\underline{H}$], is shown graphically as a function of the dissolved oxygen content, [$\underline{O}$], it is evident from Figure 5.2 that an inverse relationship exists. As the oxygen content of the weld metal increases, the hydrogen content of the weld metal decreases. Figure 5.2 suggests that, given a specific flux composition and oxygen content, the residual weld metal hydrogen content cannot be reduced below a certain threshold value, which is determined by the thermodynamics of the system.

The observed reduction in the weld metal hydrogen content with increasing levels of MIO in the flux cannot, however, be attributed only to an increase in oxygen concentration with higher levels of oxidizing ingredients in the flux. Additions of MIO to the flux formulation also leads to an increase in flux basicity. A more basic flux is expected to reduce the weld metal hydrogen content. The decrease in weld metal hydrogen content with an increase in the level of oxidizing ingredients in the flux can also be ascribed to the formation of a monolayer of FeO at the slag/metal interface which prevents hydrogen adsorption [38]. Hydrogen needs to be

transported through the slag in the form of OH^- ions and the number of OH^- ions in the slag determines the weld metal hydrogen content.

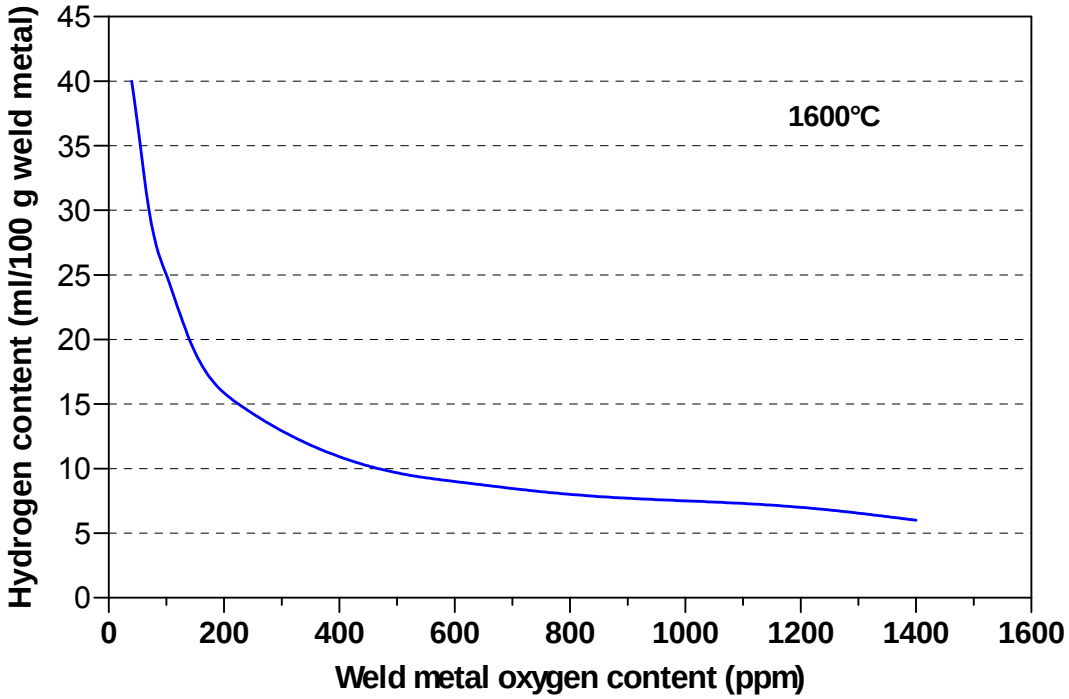

Figure 5.2 The relationship between the dissolved weld metal oxygen and hydrogen contents [11].

As shown in Figure 5.1, substitution of the iron powder in the reference flux formulation with up to 16.3% micaceous iron oxide also resulted in a reduction in the weld metal hydrogen content. Substitution of iron powder with MIO, however, has a less pronounced influence on the weld metal hydrogen level than addition of MIO, resulting in higher weld metal hydrogen contents for a given MIO content in the flux. This can be attributed to differences in the flux oxidizing ingredient content, as well as to changes in the basicity of the system. Substitution of iron powder with more than 19.3% MIO did not decrease the weld metal hydrogen content significantly. Higher levels of MIO even appeared to cause a slight increase in the diffusible weld metal hydrogen content. This increase in weld metal hydrogen at higher levels of oxidizing ingredients in the flux has also been reported by De Medeiros and Liu [39] for SMAW electrodes designed for underwater wet welding.

Although it has been shown that an increase in the level of oxidizing compounds in the flux formulation has a beneficial effect on the weld metal hydrogen content, such an increase is likely to influence the deoxidation reactions in the weld pool. An increase in oxygen content is expected to affect the partitioning of deoxidizers, particularly manganese and silicon, between the weld metal and the slag, and can potentially influence the mechanical properties of the weld metal. In order to investigate the influence of MIO additions to the flux formulation on the partitioning of deoxidizing elements between the weld metal and the slag, the likely deoxidation reactions in the weld pool were examined.

Primary deoxidation of the weld pool occurs when oxide inclusions form in the weld pool and separate from the liquid metal to gather in the slag. The original Richardson–Ellingham diagram (shown in Figure 5.3) displays the free energy of formation of various oxides as a function of temperature. The diagram suggests that silicon participates in the deoxidation of the weld pool before manganese.

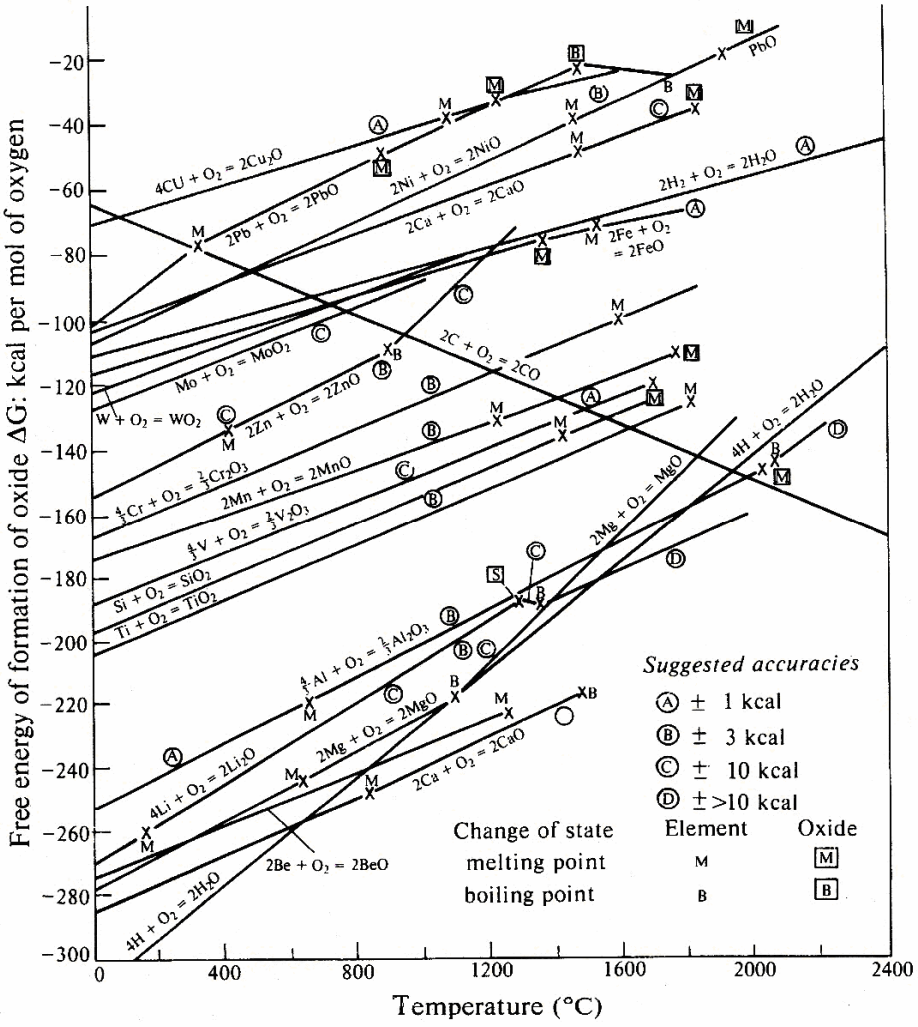

Figure 5.3 The Richardson–Ellingham diagram [40].

The same trend is evident in Figure 5.4, which shows the experimentally measured soluble oxygen concentrations for various deoxidants [16].

Grong *et al* [41] suggested that the deoxidant content of the final weld metal is controlled by reaction (5.5):

$$\underline{Si} + 2MnO = 2\underline{Mn} + SiO_2 \qquad ...(5.5)$$

Figure 5.5 compares the deoxidant (silicon and manganese) content of the weld metal with the amount of hydrogen on addition of micaceous iron oxide. Silicon declined rapidly until almost no silicon remained in the weld metal at a micaceous iron oxide content of approximately 8.8%. At higher micaceous iron oxide contents, the weld metal manganese content

decreased at a slightly faster rate as manganese became the dominant deoxidant in the weld metal. Increasing the amount of oxidizers in the flux therefore resulted in a decrease in the concentration of deoxidizers in the weld metal. The deoxidizing elements reacted with the excess oxygen and were transferred to the slag.

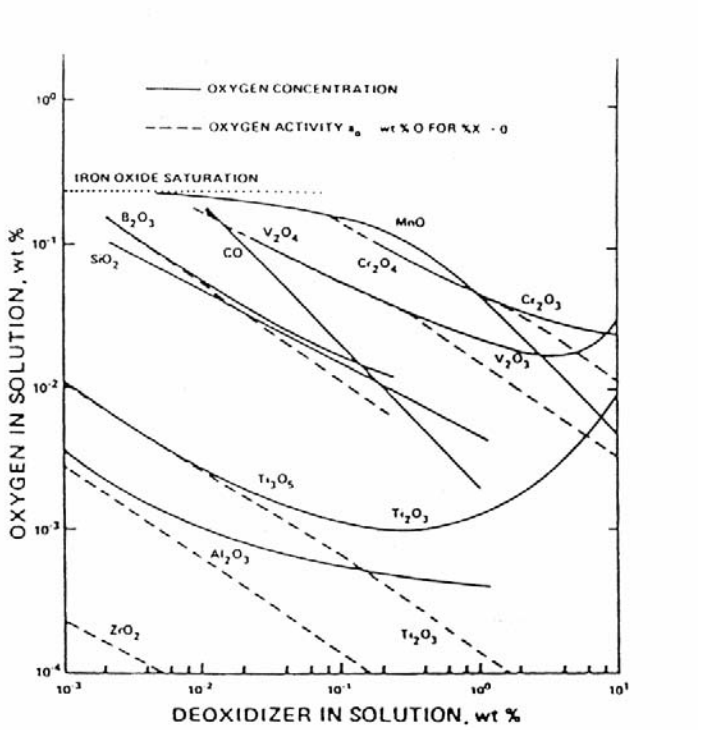

Figure 5.4 Experimentally measured soluble oxygen concentrations for various deoxidants [16].

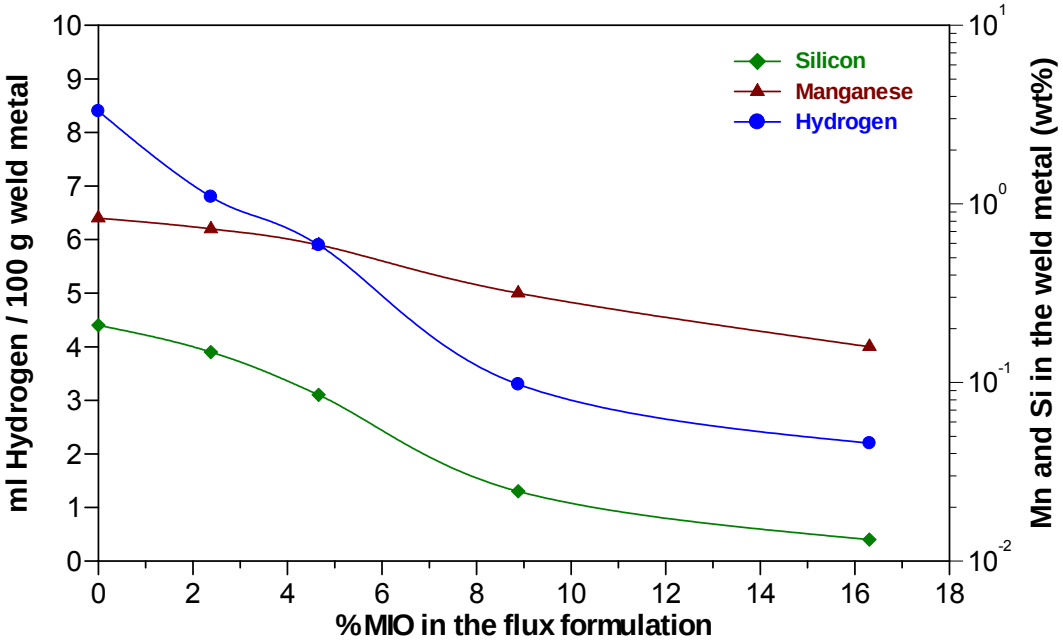

Figure 5.5 The influence of micaceous iron oxide flux additions on the deoxidant concentration in the weld metal.

Deoxidation in the weld pool on substitution of the flux iron powder by micaceous iron oxide resulted in a slightly different trend (Figure 5.6). Initially the weld metal manganese content remained almost constant and a significant decrease in silicon content was observed. At flux MIO contents greater than about 4.8%, the weld metal manganese concentration started declining as manganese becomes dominant in the deoxidation sequence.

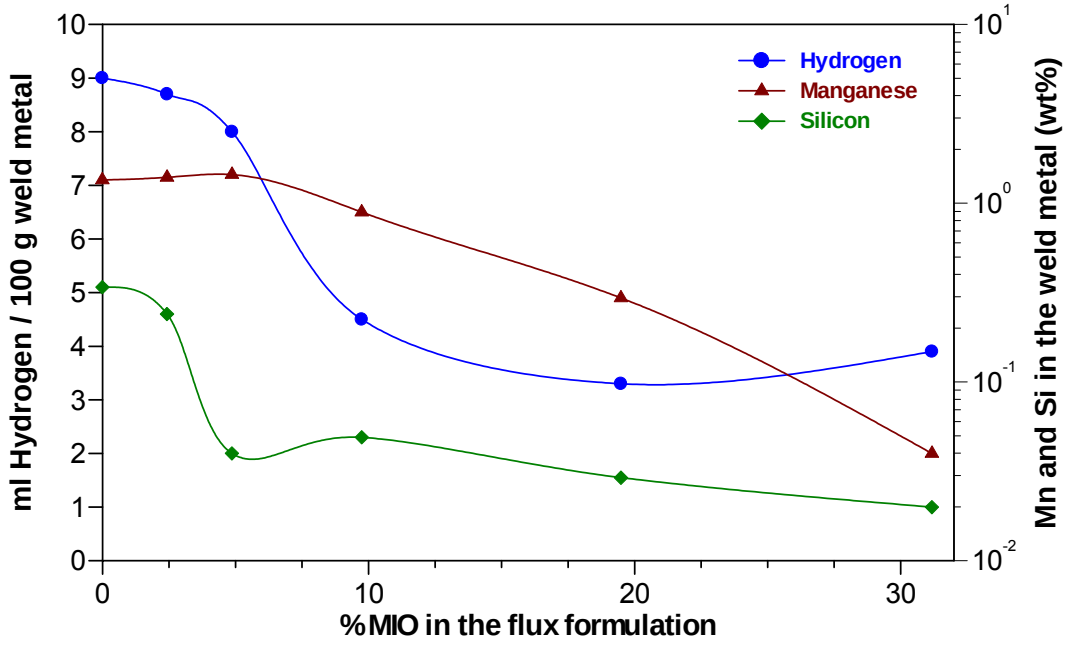

Figure 5.6 The influence of the substitution of iron powder with micaceous iron oxide in the flux formulation on the deoxidation reactions in the weld metal.

It can therefore be concluded that below a threshold concentration of oxidizing ingredients in the flux, deoxidation is primarily due to the reaction of oxygen with silicon. As the flux oxidizing content increased, more silicon was consumed. Once most of the silicon had been consumed, manganese became the dominant deoxidizer in the pool.

An attempt was also made to examine the influence of MIO additions to the reference flux formulation on the partitioning of manganese and silicon between the weld metal and the slag during welding. This was done by analysing the compositions of both the weld metal and the slag of the experimental welds. The results are considered below.

As shown in Figure 5.7, the amount of manganese in the weld metal decreased with increasing flux MIO content, whereas the amount of manganese oxide in the slag increased. This can be attributed to an increase in the oxygen content of the weld pool with an increase in flux MIO content. More manganese therefore took part in the deoxidation reaction shown in equation (5.6). The MnO formed as product of this reaction partitioned to the slag, reducing the weld pool manganese content.

$$\underline{Mn} + \underline{O} = MnO\ (slag) \qquad \ldots(5.6)$$

A similar trend was observed for the partitioning of silicon, as shown in Figure 5.8. The amount of silicon available for deoxidation in the weld pool was small compared to the amount of manganese in the experimental welds. The trend was therefore not as pronounced as that observed for manganese.

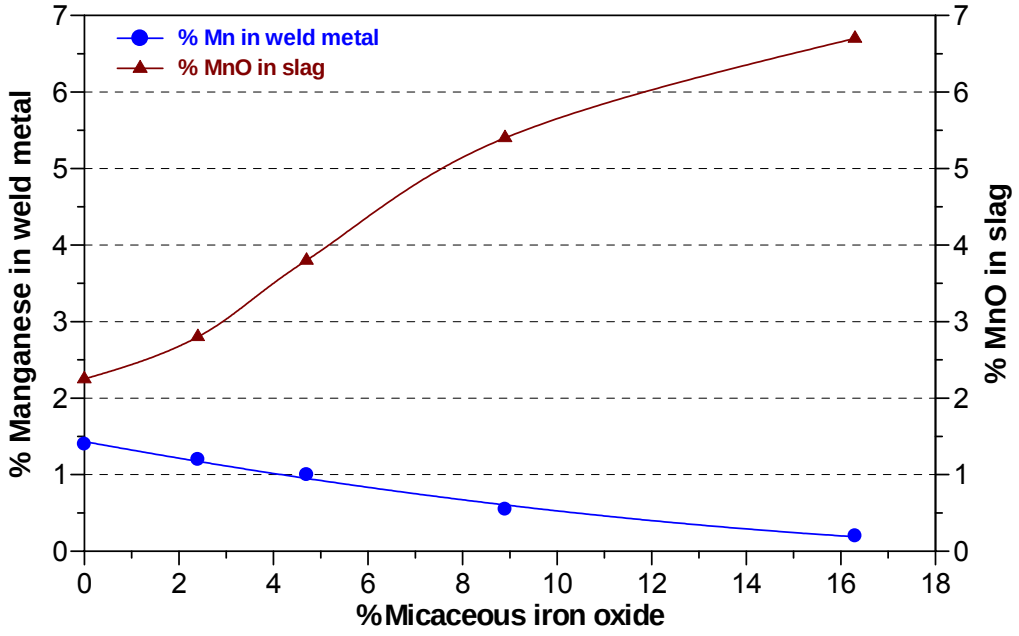

Figure 5.7 Partitioning of manganese between the weld metal and slag with the addition of micaceous iron oxide to the flux formulation.

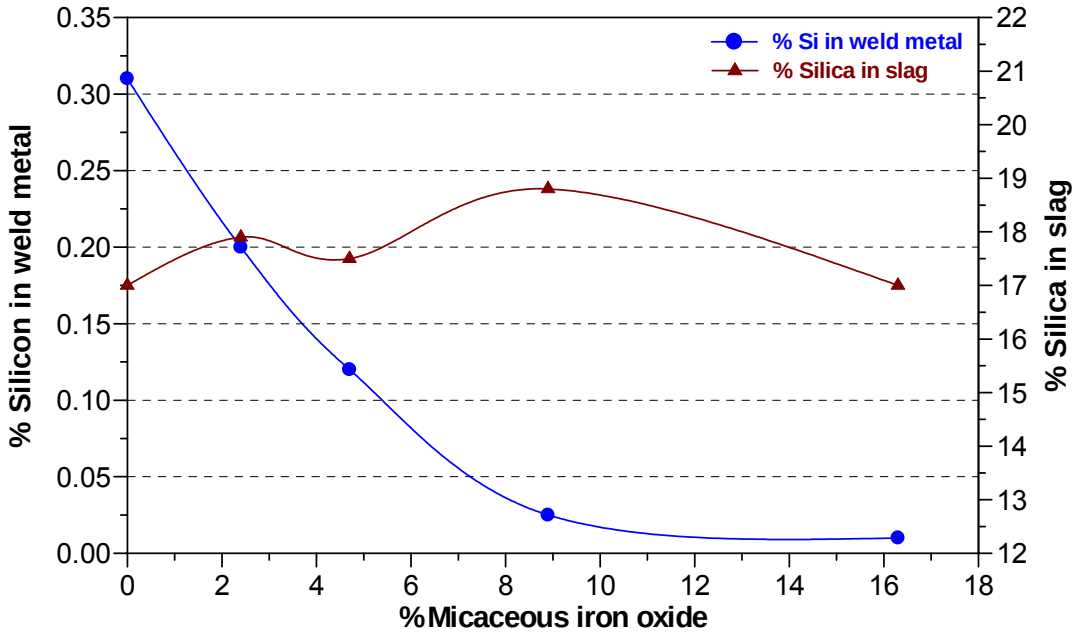

Figure 5.8 Partitioning of silicon between the weld metal and slag with the addition of micaceous iron oxide to the flux formulation.

The results obtained for MIO-containing flux formulations in this investigation revealed that MIO is beneficial in reducing diffusible weld metal hydrogen contents. This is in agreement with the proposed theory.

The addition of oxidizing ingredients to the flux therefore holds potential for the welding consumable manufacturer as a means of lowering the diffusible weld metal hydrogen content. However, one has to guard against raising the weld metal oxygen content too high as it may negatively affect the weld metal mechanical properties. Determining optimal levels of deoxidizing ingredients in the flux with respect to welding properties and weld metal mechanical properties did not form part of this investigation, and this aspect will therefore not be considered further.

5.2 THE INFLUENCE OF SILICA ADDITIONS TO THE ELECTRODE FLUX FORMULATION ON THE DIFFUSIBLE WELD METAL HYDROGEN CONTENT:

The influence of silica additions to the reference flux formulation on the diffusible hydrogen content of the experimental welds is illustrated in Figure 5.9. It is evident that the addition of silica to the electrode coating resulted in a decrease in weld metal hydrogen content. This is in direct contrast with the theory, which predicts a reduction in weld metal hydrogen content with a decrease in flux basicity.

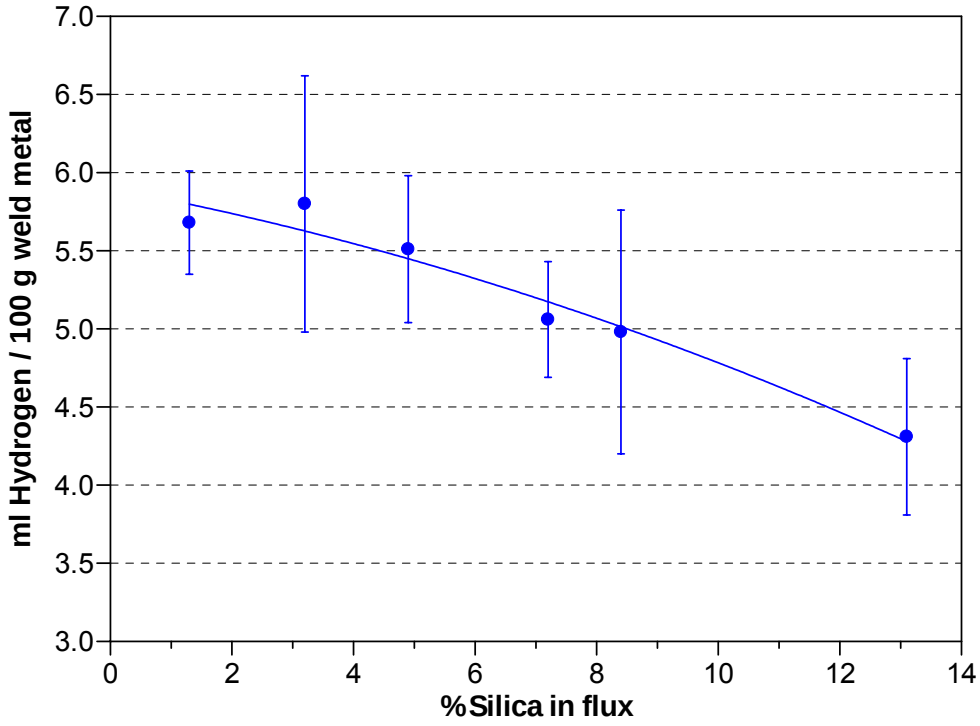

Figure 5.9 The influence of silica additions to the reference flux formulation on the diffusible weld metal hydrogen content (each data point represents the average of 7 or 8 measurements, with 95% confidence interval).

A possible explanation for this observation is that the fluorspar in the reference flux formulation reacts with silica in the flux to form SiF_4, which

functions as a shielding gas and reduces the partial pressure of hydrogen in the arc plasma [35]. This reaction is represented by equation (5.7). The CaO formed as a product of the reaction is expected to increase the basicity index of the slag, partly compensating for the expected decrease in basicity due to the presence of SiO_2. Both the reduction in hydrogen partial pressure due to the formation of SiF_4 and the formation of CaO should cause a reduction in the diffusible weld metal hydrogen levels.

$$2CaF_2 + SiO_2 \rightarrow SiF_4 + 2CaO \quad \ldots(5.7)$$

Partial dissociation of SiO_2 in the slag may also result in an increase in the amount of available oxygen. Although silica is an acidic flux, and therefore expected to dissociate only to a limited extent, the addition of high levels of SiO_2 to the flux formulation may increase the oxygen content of the weld metal sufficiently to offset the predicted increase in hydrogen content due to the decrease in basicity. As described in §5.1, an increase in the level of oxidizing ingredients in the flux formulation results in a decrease in the weld metal hydrogen content. The dominant reaction in this case is the moisture dissociation reaction, represented by equation (5.8). An increase in the weld oxygen content drives reaction (5.8) to the left, decreasing the weld metal hydrogen content.

$$H_2O_{(g)} \leftrightarrow 2H + O \quad \ldots(5.8)$$

As shown in equation (5.9), water vapour present in the form of a gaseous phase tends to react with the slag to transfer hydrogen in the form of hydroxyl ions. The slag transfers hydrogen to the liquid weld metal until equilibrium is reached.

$$H_2O + O^{2-} \rightarrow 2OH^- \quad \ldots(5.9)$$

It has been shown that water vapour behaves like an amphoteric oxide in slag. The hydroxyl capacity reaches a minimum at a slag composition of about unit basicity. Any further increase in flux basicity tends to increase the hydroxyl capacity. With the addition of silica, the hydroxyl capacity is expected to decrease, which in turn should result in lower weld metal hydrogen contents.

5.3 THE INFLUENCE OF FLUORIDE-CONTAINING COMPOUNDS ON THE DIFFUSIBLE WELD METAL HYDROGEN CONTENT:

As described in §4.2.3, a number of fluoride-containing compounds were added to the reference flux formulation to determine the effectiveness of these compounds in lowering the weld metal hydrogen content. The results of these experiments are considered below.

5.3.1 The influence of fluorspar (CaF_2) additions to the reference flux formulation:

As described in Chapter 4, the amount of fluorspar in the flux formulation was varied from 0% to 33% by weight. The measured weld metal hydrogen contents are shown in Figure 5.10. It is evident that the diffusible weld metal hydrogen content decreased with increasing levels of CaF_2 in the flux up to additions of approximately 22% fluorspar. The addition of 22% fluorspar to the formulation reduced the average weld metal hydrogen content by about 30%, compared to the hydrogen content of a formulation with no fluorspar. Above approximately 22% fluorspar, further additions of CaF_2 demonstrated little benefit. In fact, the weld metal hydrogen content seemed to increase at higher levels of fluorspar in the electrode coating.

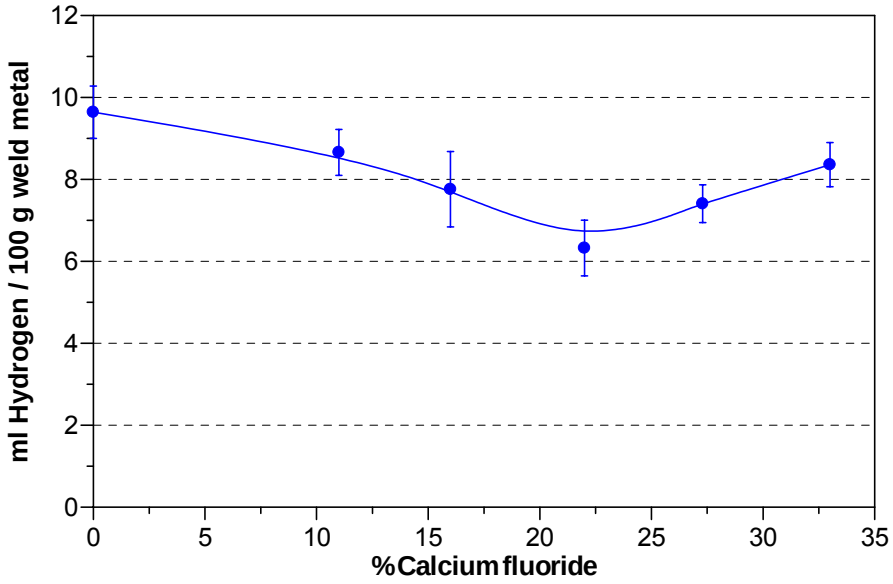

Figure 5.10 The influence of fluorspar (CaF_2) additions to the reference flux formulation on the weld metal hydrogen content (each data point represents the average of 5 or 6 measurements, with 95% confidence interval).

In the absence of high levels of SiO_2 in the flux, the dominant hydrogen removal reaction due to CaF_2 is represented by equation (5.10).

$$F_2 + H_2 \leftrightarrow 2HF \qquad \ldots(5.10)$$

The HF compound is insoluble in the weld metal, and is assumed to escape into the atmosphere during welding. This results in a reduction in the weld metal hydrogen content. An increase in fluorspar content is also expected to increase the flux basicity (as shown in equation (2.3)). An increase in flux basicity should result in a decrease in the weld metal hydrogen content. The results displayed in Figure 5.10 are therefore in agreement with predicted theory up to a fluorspar content of approximately 22%.

5.3.2 The influence of sodium fluoride (NaF) in the flux formulation on the diffusible hydrogen content of the weld metal:

As described in Chapter 4, sodium fluoride was added to the base flux formulation in amounts ranging from 0% to approximately 8.9% by weight. The results of the weld metal hydrogen measurements are given in Figure 5.11. Additions of NaF to the flux formulation resulted in an appreciable decrease in the weld metal hydrogen content. With the addition of approximately 8.9% sodium fluoride to the base formulation, the weld metal hydrogen content was observed to decrease by approximately 40%. The mechanism of hydrogen reduction through the addition of NaF is similar to that described earlier for CaF_2. Sodium fluoride dissociates in the arc to form fluorine and sodium ions. The fluorine reacts with hydrogen to form insoluble HF, thereby reducing the weld metal hydrogen content.

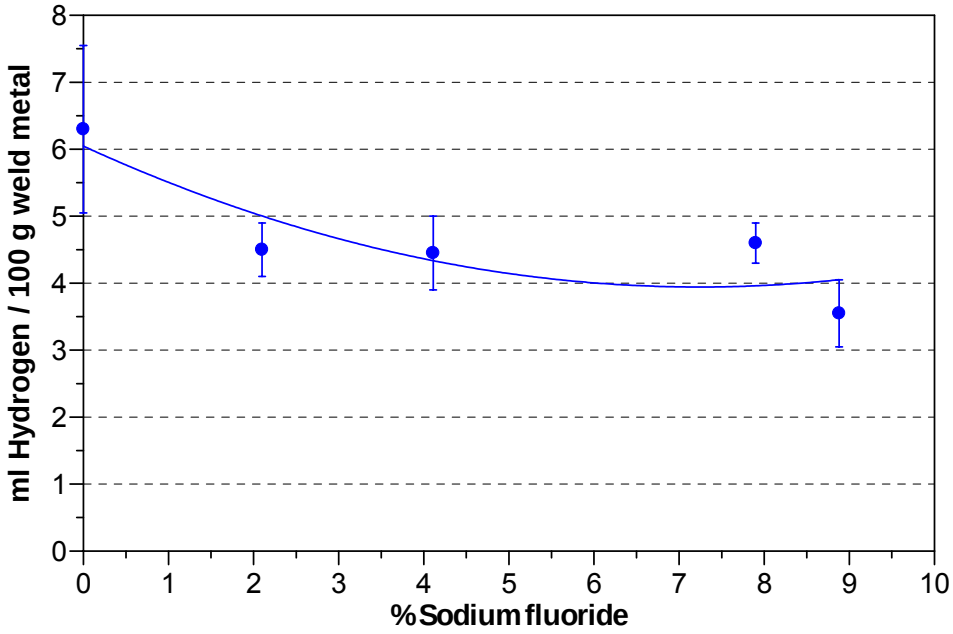

Figure 5.11 The influence of sodium fluoride (NaF) additions to the reference flux formulation on the measured weld metal hydrogen content (with 95% confidence interval).

In a separate experiment, the fluorspar contained in the base formulation was progressively substituted with sodium fluoride, keeping the sum total of the CaF_2 and NaF contents in the formulation constant at approximately 21.6%. Fluorspar dissociates poorly in the arc and therefore does not release large quantities of fluorine into the arc to react with hydrogen. Sodium fluoride dissociates more readily and releases more fluorine, which is available to react with any hydrogen present. The results of the substitution experiments are displayed in Figure 5.12. It is evident that total replacement of fluorspar with sodium fluoride may be slightly beneficial in terms of reducing the weld metal hydrogen content.

As shown in Figure 5.12, a 20% substitution of fluorspar with sodium fluoride resulted in a reduction of approximately 25% in the weld metal hydrogen content, as compared to a flux formulation with no NaF. This is

as a result of the presence of sodium fluoride, which dissociates more readily in the arc than fluorspar, releasing more fluorine to react with hydrogen.

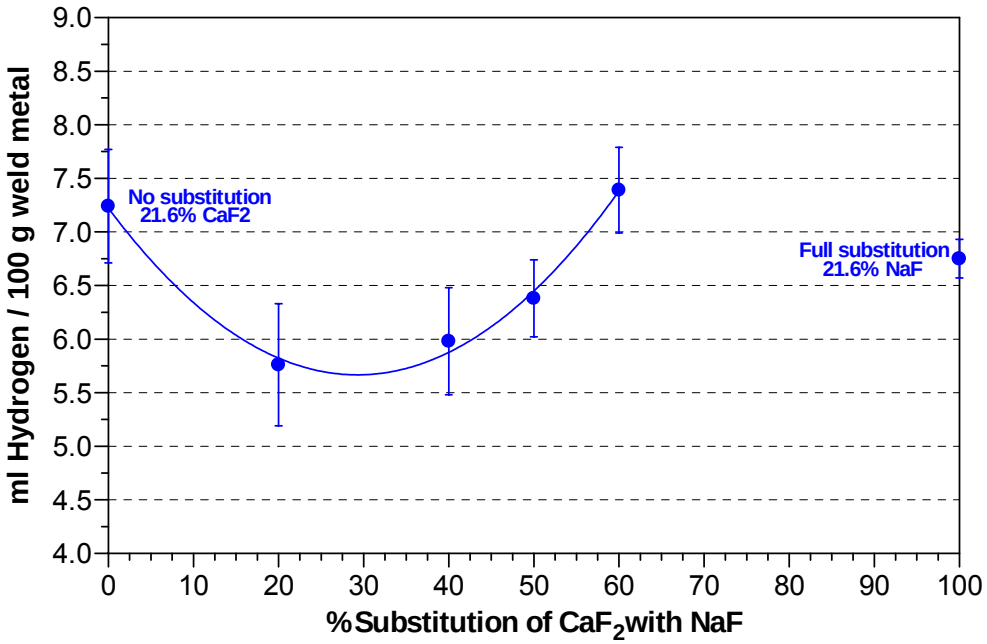

Figure 5.12 The influence of progressive substitution of fluorspar with sodium fluoride on the diffusible weld metal hydrogen content (each data point represents the average of between 5 and 9 measurements, with 95% confidence interval).

Substitution of up to 50% resulted in average weld metal hydrogen levels below those obtained with no substitution. With more than 20% substitution, however, the measured weld metal hydrogen contents exceeded those measured with no substitution of CaF_2 with NaF. This can be attributed to a reduction in the total molar amount of fluorine present in the flux. Although sodium fluoride dissociates more easily than fluorspar, it only contains half the amount of fluorine.

5.3.3 The influence of K_2TiF_6 additions to the reference flux formulation on the weld metal hydrogen content:

K_2TiF_6 was added to the reference flux formulation to determine its effectiveness in reducing the weld metal hydrogen content. K_2TiF_6 was added to the reference formulation in amounts of 2.1% and 4.7%. The results obtained for these formulations are displayed in Figure 5.13. The addition of 2.1% K_2TiF_6 resulted in a decrease of approximately 30% in the measured weld metal hydrogen content. This decrease can be attributed to more fluorine being available to react with hydrogen to form insoluble HF compounds. The base formulation contains 2.85 moles of fluorine as CaF_2. Adding 2.1% of K_2TiF_6 increased the molar amount of fluorine to 2.95. A further increase in K_2TiF_6 to 4.65% increased the amount of fluorine to 3.05 moles, but resulted in an increase in the weld metal hydrogen level.

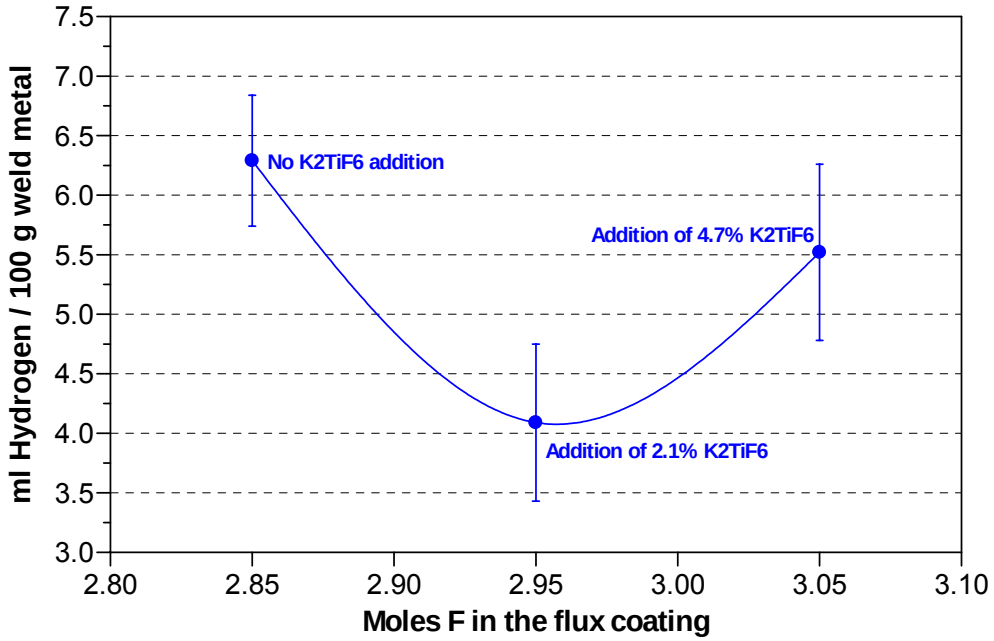

Figure 5.13 The influence of additions of K_2TiF_6 to the reference flux formulation on the measured weld metal hydrogen content (each data point represents the average of 7 measurements, with 95% confidence interval).

5.3.4 The influence of K_2AlF_6 additions to the reference flux formulation on the weld metal hydrogen content:

K_2AlF_6 was added to the base flux formulation in amounts of 4.7% and 8.9%, resulting in a slight increase in the weld metal hydrogen content. This is contrary to theoretical predictions that more fluorine should be available in the presence of K_2AlF_6 to react with hydrogen to reduce the weld metal hydrogen content. The addition of K_2AlF_6 increases the total molar amount of fluorine, and results in a larger fraction of easily dissociated fluoride-containing compounds in the flux. Matsushita and Liu [4] described a similar trend with the addition of K_2AlF_6 to flux cored wires. These authors reported a decrease in weld metal hydrogen content with the addition of up to 5% K_2AlF_6. At higher levels of K_2AlF_6 in the flux, no further decrease and even a slight increase in hydrogen content were observed.

If, instead of merely adding K_2AlF_6 to the formulation, the fluorspar in the reference formulation is substituted with K_2AlF_6, the total molar amount of fluorine present in the flux decreases, as shown in Figure 5.14. Substitution of fluorspar with K_2AlF_6 resulted in an increase in weld metal hydrogen content, as demonstrated in Figure 5.15. Given that the total molar amount of fluorine available to react with hydrogen decreases, this increase in hydrogen content in the event of substitution of CaF_2 with K_2AlF_6 is consistent with theoretical predictions.

The cost of complex fluoride-containing compounds such as K_2AlF_6 and K_2TiF_6 may be prohibitive compared with that of readily available compounds such as NaF and CaF_2. Unless the use of these compounds results in a dramatic decrease in the weld metal hydrogen content (not

observed in this investigation), it would not be economically feasible to use K_2AlF_6 and K_2TiF_6 as flux additives during the commercial production of basic SMAW electrodes.

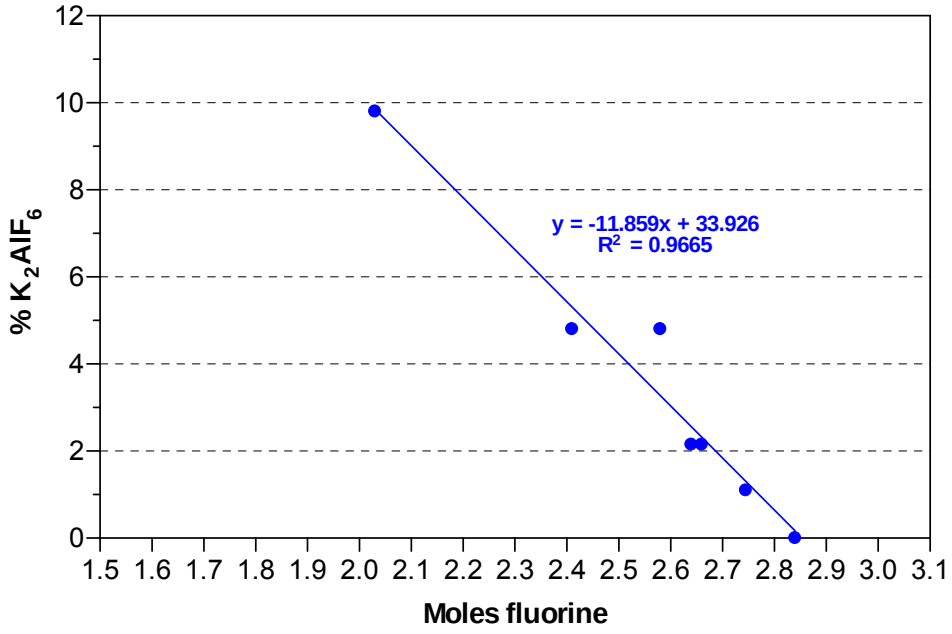

Figure 5.14 The influence of substitution of CaF_2 with K_2AlF_6 on the molar amount of fluorine available in the flux.

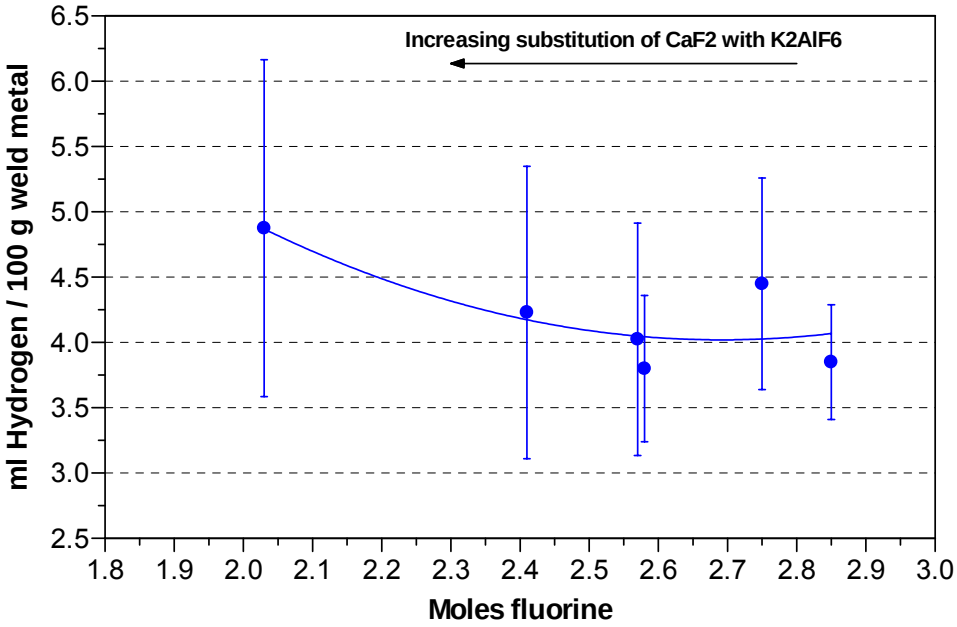

Figure 5.15 The influence of progressive substitution of fluorspar with K_2AlF_6 on the measured weld metal hydrogen content (each data point represents the average of between 3 and 7 measurements, with 95% confidence interval).

5.4 THE INFLUENCE OF CALCITE ($CaCO_3$) ADDITIONS TO THE REFERENCE FLUX FORMULATION ON THE DIFFUSIBLE WELD METAL HYDROGEN CONTENT:

In order to investigate the influence of calcite additions to the reference flux formulation on the diffusible weld metal hydrogen content, the percentage calcite in the flux was varied from 10% to almost 24%. The base formulation normally contains approximately 16% calcite. In the first set of experiments, no attempt was made to balance the flux formulation, and only the amount of calcite added to the flux formulation was varied. In the second set of experiments, the amount of calcite in the flux formulation was balanced by varying the amount of iron powder in the formulation.

Both sets of experiments showed similar trends, as illustrated in Figure 5.16. An increase in calcite content initially gave rise to a reduction in the weld metal hydrogen content, but this trend appeared to reverse at higher levels of calcite. Balancing the formulation with iron powder, compared to merely adding calcite, resulted in the hydrogen curve being shifted to lower hydrogen levels. This can be ascribed to an increase in the weld metal oxygen content, which resulted in a decrease in the weld metal hydrogen content.

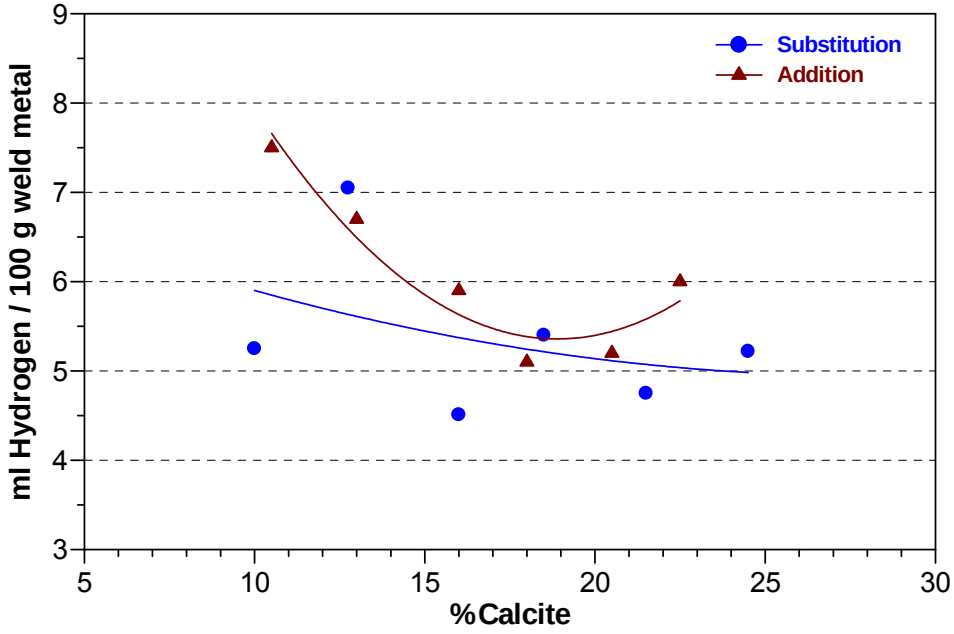

Figure 5.16 The influence of the calcite content of the flux formulation on the diffusible weld metal hydrogen content (each data point represents the average of 32 measurements).

As shown in Figure 5.17, the relationship between calcite additions and the weld metal hydrogen content appeared to be largely linear up to about 18% calcite in the flux formulation. This relationship between calcite content and weld metal hydrogen level within this concentration range corresponds to the mathematical formula shown in equation (5.11).

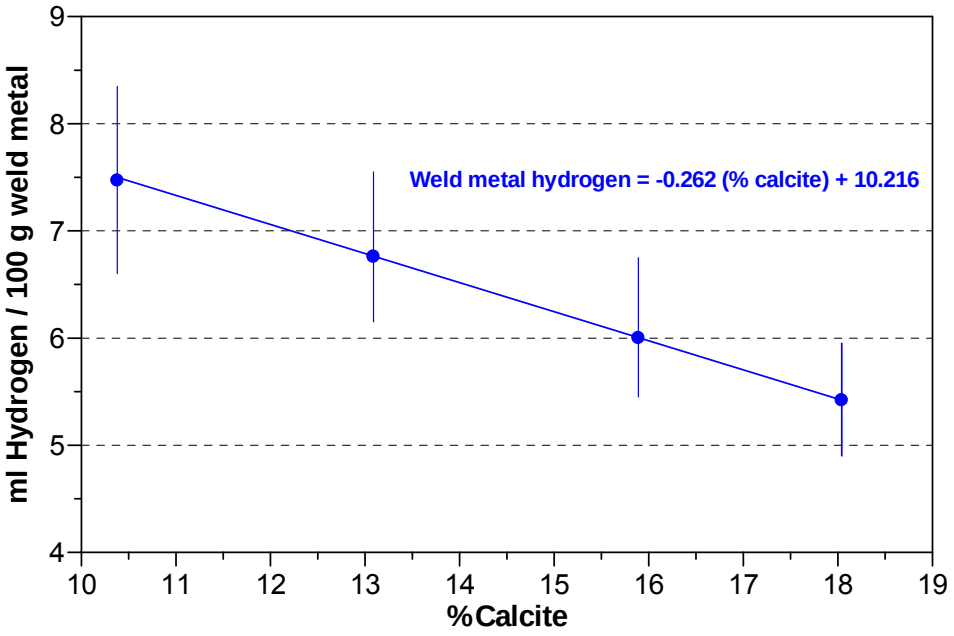

Figure 5.17 The relationship between calcite flux additions (up to 18% calcite) and the diffusible weld metal hydrogen content (with 95% confidence interval).

H-content = -0.262 (%calcite in the flux) + 10.216 ...(5.11)

This formula predicts a weld metal hydrogen content of 10.2 ml/100 g weld metal with no calcite addition to the flux formulation. This value could not be experimentally verified as the electrode displayed poor arc stability and inadequate shielding without any calcite addition.

With further additions of calcite (above 18%), the weld metal hydrogen content increased, as shown in Figure 5.18. This suggests that the decomposition of calcite in the welding arc was no longer the dominant reaction controlling the absorption of hydrogen.

The influence of calcite additions to the flux formulation on the weld metal oxygen content is illustrated in Figure 5.19. As shown in equations (5.12) and (5.13), calcite decomposes in the arc to form CaO, CO and CO_2.

$$CaCO_3 \leftrightarrow CaO + CO_2 \quad ...(5.12)$$

$$2CO_2 \leftrightarrow 2CO + O_2 \quad ...(5.13)$$

CaO increases the basicity of the slag system, which should result in a decrease in the amount of weld metal hydrogen. The presence of CO and CO_2 in the arc atmosphere reduces the partial pressure of hydrogen, which should also reduce the diffusible weld metal hydrogen content. As shown in Figure 5.19, the weld metal oxygen content remained relatively stable with additions of up to 18% calcite to the flux formulation. Further additions of calcite resulted in an increase in the weld metal oxygen content. This increase in weld metal oxygen content coincides with the observed

increase in weld metal hydrogen content with additions of more than 18% calcite to the flux formulation.

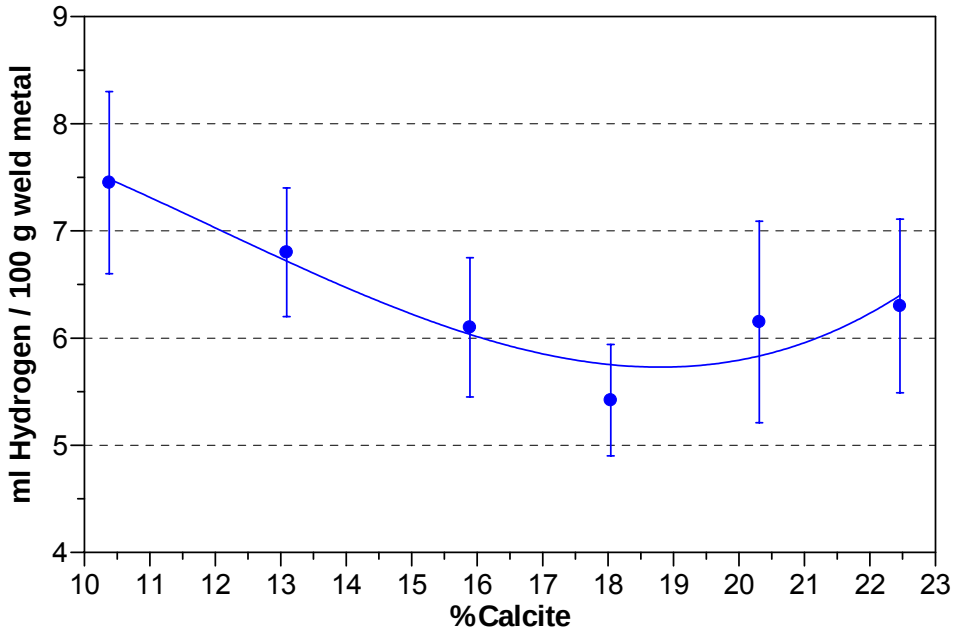

Figure 5.18 The influence of calcite additions to the flux formulation on the diffusible weld metal hydrogen content (with 95% confidence interval).

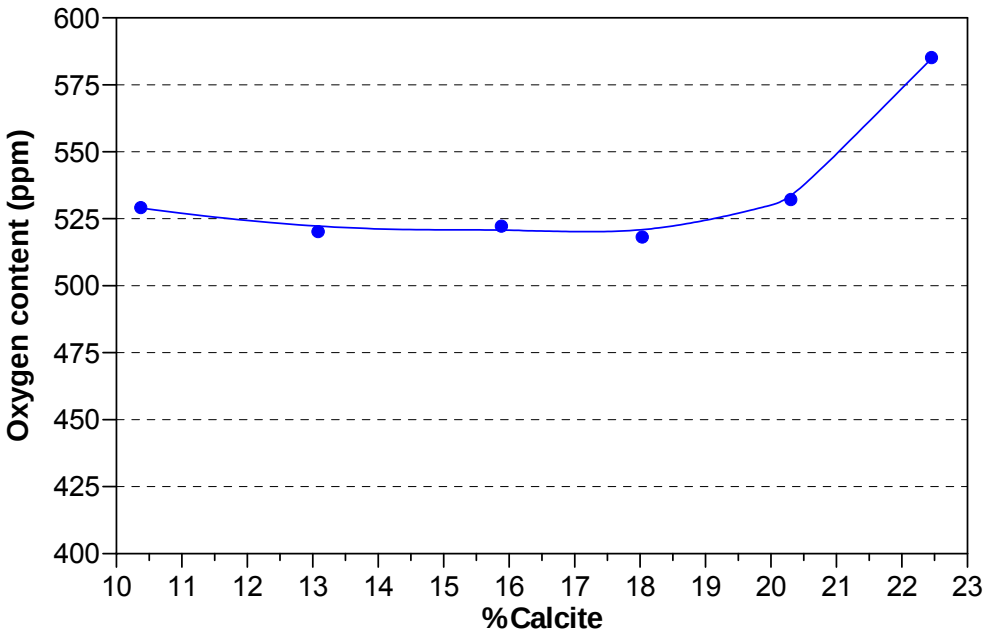

Figure 5.19 The influence of calcite additions to the flux formulation on the weld metal oxygen content.

These results suggest that there are a number of competing mechanisms determining the weld metal hydrogen content. Although it is difficult to isolate the individual contributions of the different mechanisms which

control the weld metal hydrogen content, an attempt will be made in the next paragraph to understand the individual reactions that occur in the arc and weld metal by examining the partitioning of elements between the weld metal and the slag.

5.4.1 Analysis of the welding slag:

In order to examine the partitioning of elements between the weld metal and the slag, the slag layers formed during welding using three of the experimental calcite-containing electrodes were collected. The flux formulations for these electrodes contained 10.38%, 18.04% and 22.46% calcite, respectively, representing "low", "medium" and "high" calcite concentrations. The typical flux compositions of the three electrodes are given in Table 5.1. The collected slag was mounted in resin, polished and analyzed using the EDS-facility of a scanning electron microscope (SEM). The concentration of the different oxides in the slag was calculated from the composition.

Table 5.1 Flux compositions of three experimental electrodes, containing "low", "medium" and "high" calcite contents (percentage by weight).

Raw material	Electrode designation		
	C1058 Low calcite	**C1055 Medium calcite**	**C1059 High calcite**
Ferrosilicon	2.80%	2.56%	2.43%
Fluorspar, CaF_2	23.05%	21.08%	19.95%
Rutile, TiO_2	5.61%	5.13%	4.85%
Sodium fluoride, NaF	5.71%	5.22%	4.94%
Carbonate	10.38%	18.04%	22.46%
Manganese	3.74%	3.42%	3.23%

A typical SEM-EDS spectrum for the slag is shown in Figure 5.20.

The following observations were made from the SEM-EDS analyses of the slag:

- Higher levels of fluorspar, CaF_2, in the flux formulation resulted in more fluorine in the slag, as shown in Figure 5.21.
- As shown in Figure 5.22, higher levels of calcite in the flux resulted in more CaO in the slag.
- The levels of manganese oxide and silica in the slag are indicative of the extent of deoxidation in the weld pool.

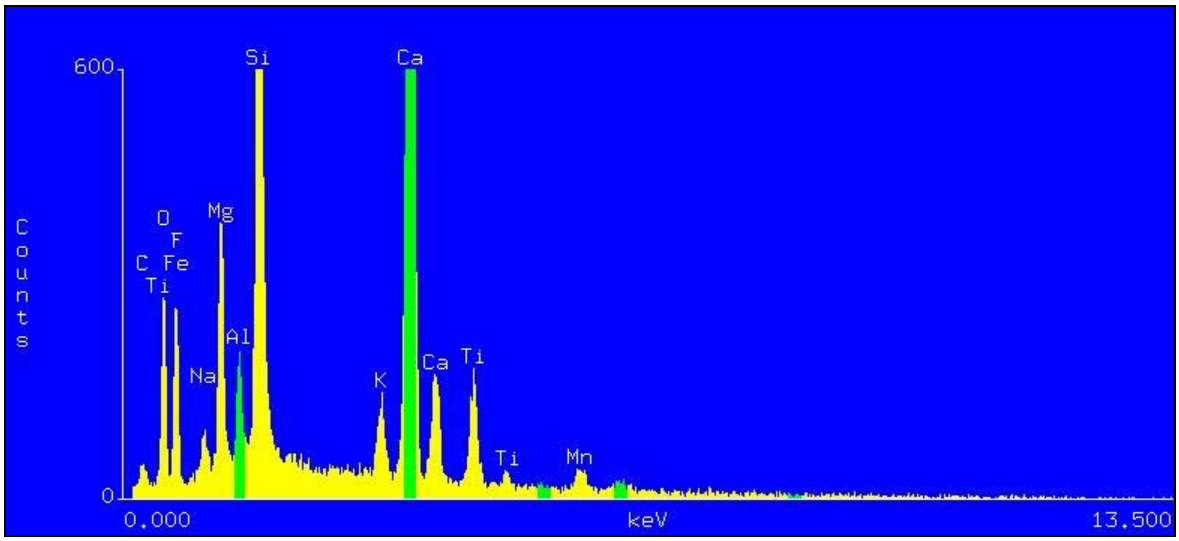

Figure 5.20 A typical SEM-EDS spectrum of the slag of weld C1055 (medium calcite content).

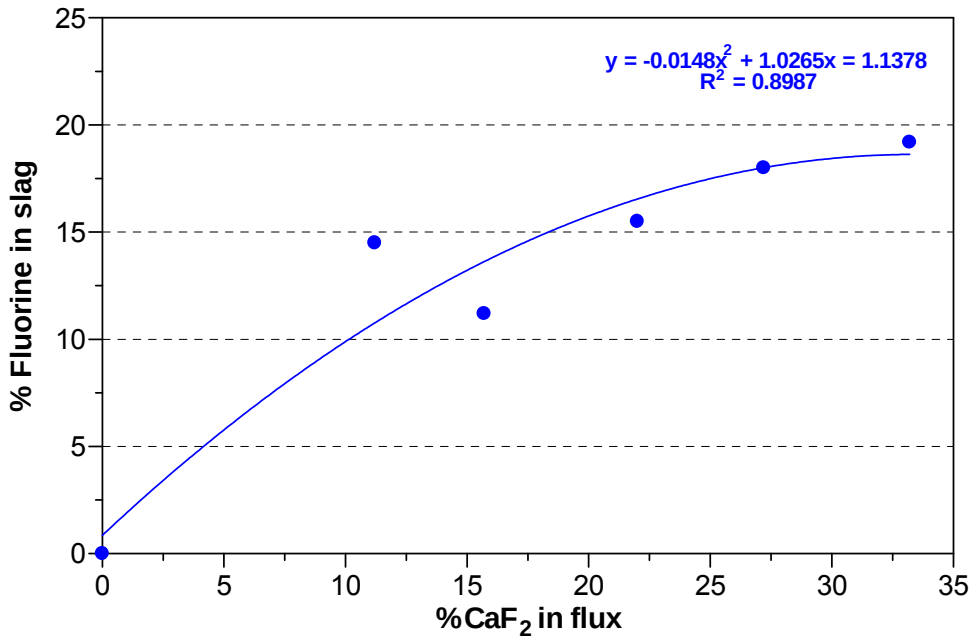

Figure 5.21 Comparison between the fluorine content of the slag and the amount of fluorspar in the electrode flux formulation.

As shown in Figures 5.23 and 5.24, the slag samples were not found to consist of a homogeneous glassy phase, as expected, but were shown to consist of a matrix phase, a fine dendritic substructure, and a number of larger dendrites (shown in Figure 5.24). Different volume fractions of the dendritic phase were observed in the three slag samples examined.

In order to identify the phases in the slag microstructures, the matrix phase and the large dendrites were analysed. The results of the SEM-EDS analyses are given in Table 5.2.

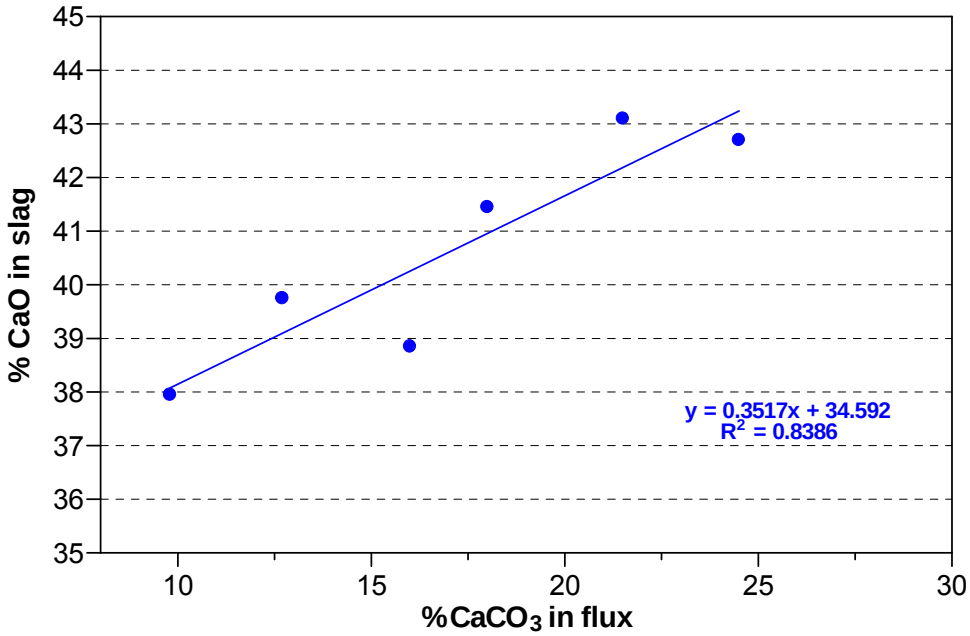

Figure 5.22 Comparison between the amount of CaO in slag and the amount of calcite in the electrode flux formulation.

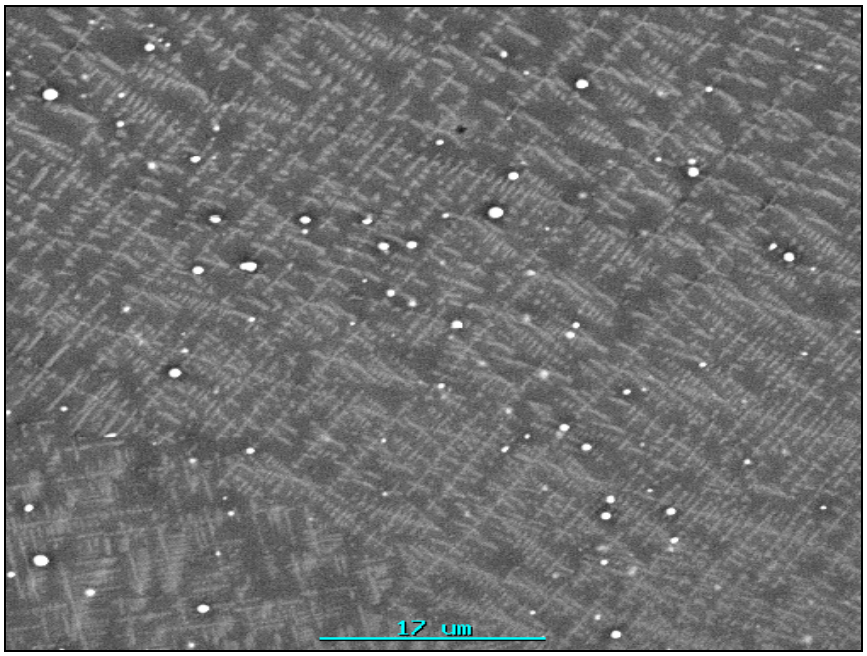

Figure 5.23 SEM micrograph of the slag of weld C1059 (high calcite content), showing a dendritic structure and a number of fine metallic droplets (magnification: 1750x).

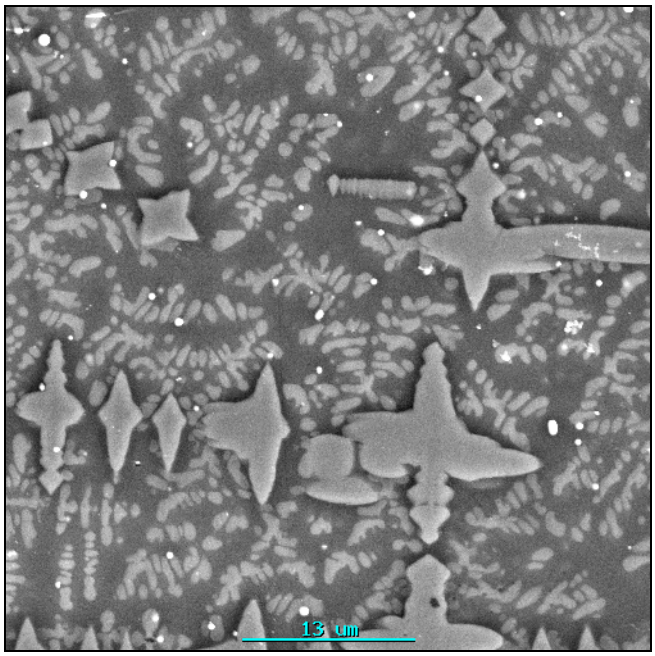

Figure 5.24 SEM micrograph of the slag of weld C1059 (high calcite content), showing a fine dendritic structure, larger dendrites and some fine metallic droplets (magnification: 1750X).

Table 5.2 SEM-EDS analyses of the matrix phase and the dendrites in the slag structure (weight percentage).

Compound	Matrix phase			Dendrite phase		
	C1058	C1055	C1059	C1058	C1055	C1059
Na_2O	0.5	1.1	1.4	0.2	NM	0.1
MgO	5.7	6.2	6.2	1.3	NM	0.9
Al_2O_3	2.1	1.8	2.4	2.1	NM	1.6
SiO_2	18.7	18.8	15.9	2.3	NM	2.1
K_2O	1.1	2.1	2.7	0.3	NM	0.3
CaO	41.8	38.5	34.6	38.8	NM	38.1
TiO_2	9.6	7.5	11.4	52.8	NM	55.0
MnO	3.3	2.9	3.0	0.1	NM	0.4
FeO	2.4	1.1	1.8	0.7	NM	0.1
F	14.9	20.0	20.4	1.5	NM	1.4

NM: not measured

The matrix phase appears to be rich in CaO, SiO_2, MgO, TiO_2 and fluorine. The chemical composition of the dendritic phase in all the slag samples examined was found to be similar, indicating that the same dendritic phase formed. The chemical composition of this primary dendritic phase differs significantly from the chemical analysis of the slag matrix. The dendritic phase is highly enriched in TiO_2 and CaO, and contains almost no silica, manganese oxide or fluorine.

The phase diagram for the CaO–TiO_2 system, after DeVries, Roy and Osborn [42], indicates that the dendritic phase is probably perovskite (see Figure 5.24). Perovskite is a very stable phase that forms on solidification, as evidenced by the dendritic structure observed in the slag samples. These results suggest that the slag was completely molten during welding.

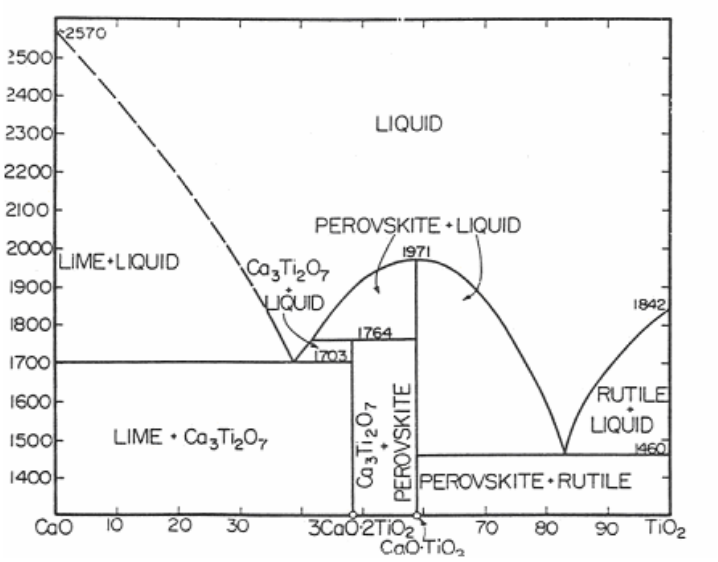

Figure 5.24 Binary phase diagram for the CaO–TiO_2 system [42].

5.4.2 Evaluation of the hydroxyl capacity and optical basicity of the slag:

In order to explain the tendency of the weld metal hydrogen content to pass through a minimum on addition of fluoride-containing compounds and calcite to the electrode flux formulation, the hydroxyl capacity and the optical basicity of a number of experimental SMAW flux formulations were calculated. The CaF_2 content in these formulations varied from 0% to 33.22%, and the $CaCO_3$ content from 10.38% to 22.46%. The approximate compositions of these flux formulations are given in Table 5.3.

After welding, the weld metal composition and the slag chemistry of each of the welds were determined. The measured slag compositions are shown in Table 5.4. The optical basicity and the hydroxyl capacity of each slag were then calculated from equations (1.15), (1.16), (2.4) and (2.6). The following sequence of calculations was used to determine the optical basicity and the hydroxyl capacity of each slag chemistry shown in Table 5.4:

- calculation of the molar amount of each slag component,
- calculation of the activity coefficients,
- calculation of the optical basicity of the slag, and
- calculation of the hydroxyl or water capacity of the slag.

The results of these calculations are presented in Table 5.5, and illustrate the relationship between optical basicity, water capacity, slag chemistry and the as-deposited weld metal hydrogen content.

Table 5.3 The raw material ingredients added to twelve experimental flux formulations (weight percentage).

Sample number	Ferro-silicon	CaF_2	TiO_2	Feldspar	Carbonate	Fe-powder	Mn
C1054	2.63	21.64	5.26	5.36	15.89	31.19	3.51
C1055	2.56	21.08	5.13	5.22	18.04	30.39	3.42
C1056	2.49	20.50	4.99	5.08	20.31	29.55	3.32
C1057	2.72	22.36	5.44	5.54	13.09	32.23	3.63
C1058	2.80	23.05	5.61	5.71	10.38	33.23	3.74
C1059	2.43	19.95	4.85	4.94	22.46	28.75	3.23
C2006	2.63	21.64	5.26	5.36	15.89	31.19	3.51
C2007	3.36	0.0	6.72	6.84	20.27	39.80	4.48
C2008	2.99	11.06	5.97	6.08	18.03	35.40	3.98
C2009	2.83	15.72	5.66	5.77	17.09	33.54	3.77
C2010	2.45	27.17	4.89	4.89	14.76	28.99	3.26
C2011	2.24	33.22	4.49	4.57	13.54	26.58	2.99

Table 5.4 Chemical analysis of the slag constituent of each weld, determined using wet chemistry methods (weight percentage).

Sample number	SiO_2	Al_2O_3	Total Fe	Metallic Fe	TiO_2	CaO	MgO	K_2O	MnO	F
C1054	18.1	2.20	2.31	0.69	9.49	38.8	5.77	2.20	2.21	13.5
C1055	19.3	2.24	2.29	0.58	9.50	41.4	5.92	2.28	2.37	13.5
C1056	17.4	2.19	2.64	1.22	9.35	43.1	5.79	1.79	2.38	12.9
C1057	18.6	2.37	1.90	0.86	10.2	39.7	6.21	2.40	2.38	14.7
C1058	18.1	2.29	2.07	1.02	10.5	38.0	6.31	2.52	2.69	15.4
C1059	19.2	2.09	3.15	1.28	8.74	42.6	5.41	1.88	2.62	12.1
C2006	17.3	2.20	1.67	1.30	10.3	41.3	6.00	2.30	2.02	15.3
C2007	24.3	3.44	6.94	2.94	16.4	23.4	9.19	2.59	5.12	0.20
C2008	17.9	2.31	3.52	2.56	9.34	41.7	5.65	1.90	2.35	14.6
C2009	20.2	2.69	2.75	2.25	11.2	36.8	6.44	2.17	2.39	11.1
C2010	14.1	1.78	2.34	1.62	8.94	44.1	5.27	1.89	1.85	18.1
C2011	12.6	1.58	2.49	2.31	7.44	46.7	4.55	1.96	1.62	19.5

Higher levels of $CaCO_3$ in the flux cause the amount of CaO in the slag to increase (samples C1054 to C1059). This leads to an increase in the optical slag basicity, resulting in an increase in the slag water capacity (shown in Figure 5.25). The effect of additions of CaF_2 to the flux formulation (samples C2006 to C2011) is less evident, due to variations in both the $CaCO_3$ content (from 13.54% to 20.27%) and the CaF_2 content (from 0% to 33.22%) of these flux formulations. As described in §2.2, a minimum in water vapour solubility has been reported near neutral basicity

in many slag systems. When the slag water capacity, calculated from equation (2.6), is shown graphically as a function of the optical basicity, however, the minimum is observed to occur at an optical basicity of approximately 0.6 (Figure 5.26).

Table 5.5 The calculated values of the optical basicity, Λ, and the water capacity, C_{H_2O} (ppm/($P_{H_2O}^{0.5}$)), of various slag chemistries.

Sample number	Optical basicity, Λ	log C_{H_2O}	C_{H_2O}	Weld metal hydrogen content
C1054	0.7472	3.1595	1443.742	5.8 ml/100 g
C1055	0.7486	3.1666	1467.737	4.8 ml/100 g
C1056	0.7600	3.2283	1691.585	5.7 ml/100 g
C1057	0.7467	3.1568	1434.903	6.2 ml/100 g
C1058	0.7456	3.1512	1416.292	7.5 ml/100 g
C1059	0.7525	3.1872	1538.956	5.5 ml/100 g
C2006	0.7559	3.2058	1606.128	6.3 ml/100 g
C2007	0.6804	2.8963	787.599	9.6 ml/100 g
C2008	0.7542	3.1964	1571.738	8.6 ml/100 g
C2009	0.7290	3.0716	1179.344	7.8 ml/100 g
C2010	0.7820	3.3606	2294.128	7.4 ml/100 g
C2011	0.8016	3.4919	3104.166	8.4 ml/100 g

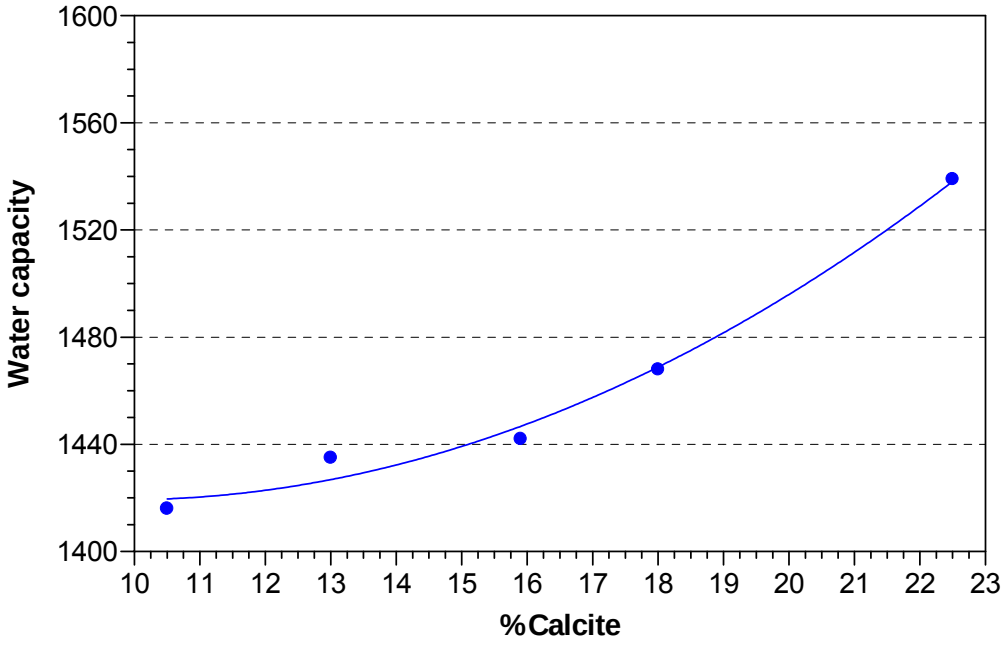

Figure 5.25 The relationship between the flux $CaCO_3$ content and the calculated water capacity of the slag (ppm/$atm^{0.5}$).

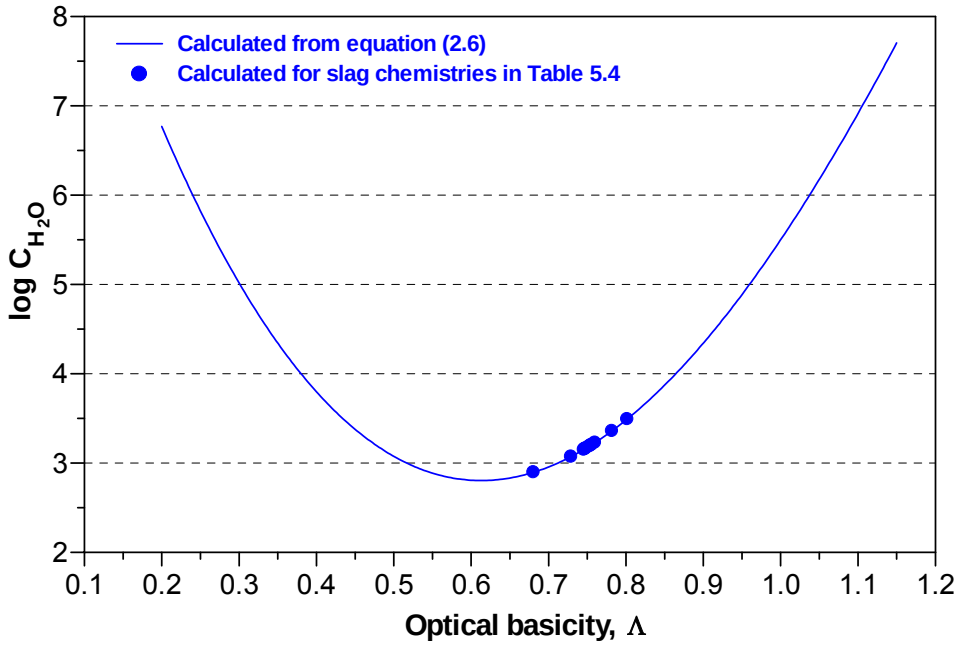

Figure 5.26 The slag water capacity, calculated from equation (2.6), as a function of the optical basicity, including data points representing the experimental slag chemistries (from Table 5.4).

Also shown in Figure 5.26 are data points representing the calculated water capacity and optical basicity of each of the slag chemistries shown in Table 5.4. These values are all located in the vicinity of the minimum in slag water capacity, but the results shown in this figure still do not account for the minima observed in the diffusible weld metal hydrogen contents with the addition of fluoride-containing compounds and $CaCO_3$ to the flux.

The correlation between the optical basicity and the slag water capacity shown in Figure 5.26 originated from results for binary and ternary slags containing CaO, SiO_2, MgO and Al_2O_3. The slag chemistries shown in Table 5.4 are, however, considerably more complex and this may influence the relationship between the basicity and the slag water capacity. For better prediction in the present case, the slag model "FACT-SLAG?" of FACTSage was used. The model considered the slag as a solution of the species SiO_2, TiO_2, CaO, FeO, Na_2O, Al_2O_3, MgO, NaF, CaF_2, MgF_2, FeF_2, H_2O, NaOH, $Ca(OH)_2$, $Mg(OH)_2$ and $Fe(OH)_2$. The slag was conceptually equilibrated with a large excess of gas containing 1% (by volume) H_2O in Ar. The calculated total water content of the slag (as hydroxide or dissolved water) was then used to calculate the water capacity, C_{H_2O}, from equation (5.14). Since not all the species present in the welding slag are included in the slag model, some substitutions had to be made. For this calculation, MnO was included in the calculation as an equivalent amount (mole for mole) of FeO, SrO was included as CaO, and K_2O as Na_2O.

$$C_{H_2O} = \frac{ppm\ \ H_2O}{\sqrt{P_{H_2O}}} \qquad \ldots(5.14)$$

In order to highlight the predictions of the model, Figure 5.27 displays the calculated water capacity as a function of slag basicity and fluoride content. In this figure, the basicity (B) is given by (%CaO)/(%SiO_2), where "CaO" refers to the total calcium content of the slag (whether present as CaO or as CaF_2). Figure 5.27 illustrates that the slag water capacity is a strong function of the slag basicity, with an increase in basicity resulting in higher slag water capacities for the range of chemistries evaluated. The slag water capacity is, however, also determined by the slag fluorine content. At a constant basicity, substitution of CaO with CaF_2 (resulting in an increase in slag fluorine content) decreases the water capacity.

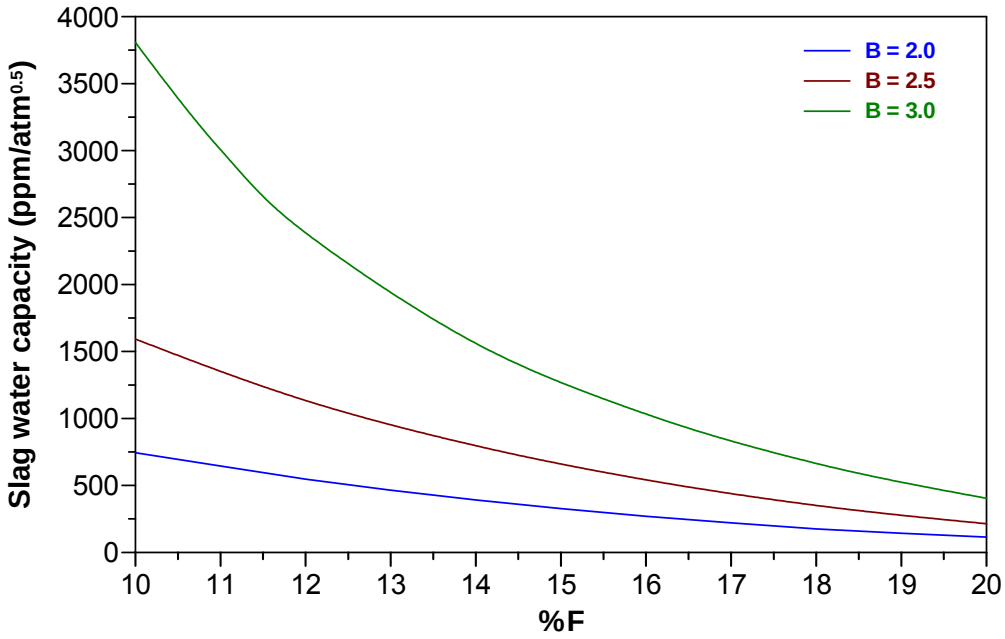

Figure 5.27 Calculated water capacity of welding slags with different fluoride contents and basicities. The basicity is (%CaO)/(%SiO_2). In addition to the variable contents of SiO_2, CaO and CaF_2, the slag was taken to contain constant mass percentages of Al_2O_3 (2%), FeO (4%), TiO_2 (11%), MgO (6%) and Na_2O (1.5%).

Although theory predicts that increasing slag basicity and higher flux CaF_2 levels should decrease the weld metal hydrogen content, Figure 5.27 illustrates that an increase in the slag fluorine content reduces the slag water capacity. This can be attributed to the relative contributions of CaF_2 and CaO towards increasing the slag basicity. Even though equation (2.3) predicts that CaF_2 increases the slag basicity to the same extent as CaO, its effect on the optical slag basicity is less pronounced (estimated Λ_{th} values for CaF_2 range from 0.43 to 0.67, compared to 1.0 for CaO [43]). The addition of CaF_2 to the flux formulation, resulting in higher levels of fluorine in the slag, therefore dilutes the beneficial effect of CaO on the slag optical basicity and water capacity. A decrease in the slag water capacity tends to increase the diffusible weld metal hydrogen content, as shown in Figure 5.28. The predicted decrease in slag water capacity with higher levels of fluorine in the slag may account for the higher weld metal

hydrogen contents observed on addition of high concentrations of fluorine-containing compounds to the flux (as shown in Figures 5.10 and 5.13).

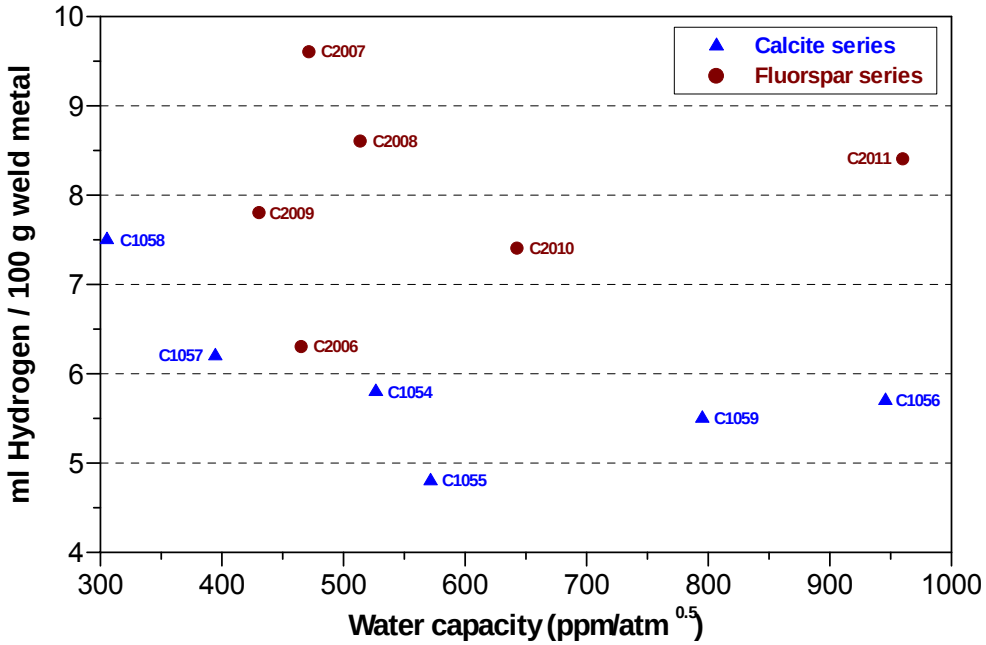

Figure 5.28 The relationship between the calculated slag water capacity (from the FACTSage slag model) and the measured weld metal hydrogen content of experimental electrodes with compositions shown in Table 5.3.

The data points labelled “calcite series” in Figure 5.28 demonstrate the influence of increasing flux calcite content (at fairly constant levels of CaF_2) on the slag water capacity and weld metal hydrogen content. Increasing additions of $CaCO_3$ to these flux formulations tend to raise the slag basicity, causing an increase in the slag water capacity and a reduction in the measured weld metal hydrogen level.

The data points in the “fluorspar” series in Figure 5.28 display considerably more scatter. This can be attributed to variations in both the $CaCO_3$ content (from 13.54% to 20.27%) and the CaF_2 content (from 0% to 33.22%) of the flux formulations, resulting in a wide range of slag basicities and fluorine contents. Although the slags in this series tend to be more basic than the slags in the calcite series (with the exception of fluxes with very low CaF_2 levels, i.e. samples C2007 and C2008), the slag water capacities are generally lower and the weld metal hydrogen contents higher. (Even though sample C2011 has a high slag fluorine content, its basicity is disproportionately high, which may account for its high water capacity). This confirms the earlier prediction that high slag fluorine levels may reduce the slag water capacity, even though CaF_2 additions to the slag are reported to raise the slag basicity.

Figure 5.28 indicates that the lowest weld metal hydrogen contents are found at flux $CaCO_3$ and CaF_2 contents that are very close to those in the current reference flux formulation. An increase in CaF_2 content with the aim of decreasing the weld metal hydrogen content is therefore not recommended in the electrodes examined.

CHAPTER 6

CONCLUSIONS AND RECOMMENDATIONS

The prevalence of hydrogen-induced cracking during the welding of ferritic steels often necessitates the use of stringent welding procedures. The methods available to the fabricator to combat hydrogen cracking are costly and time-consuming, and include the use of low hydrogen welding consumables, preheating and interpass temperature control, postweld heat treatment, and strict heat input control during welding. During shielded metal arc welding (SMAW), the preheat and interpass temperatures required to prevent hydrogen-induced cracking during welding are dependent on the hydrogen potential of the welding consumable.

An incentive therefore exists for welding consumable manufacturers to reduce the hydrogen potential of basic-type SMAW electrodes. Modification of the arc chemistry through the use of flux additions presents an attractive option. During the course of this project, a number of hydrogen reduction strategies involving arc chemistry modification were examined. Experimental shielded metal arc welding electrodes with flux formulations based on the coating composition of an E7018-1 basic-type electrode were produced, and the diffusible weld metal hydrogen contents of welds deposited using these experimental electrodes were measured. A summary of the results of this investigation is given below:

- The addition of oxidizing ingredients to the reference flux formulation (in the form of micaceous iron oxide) lowered the diffusible weld metal hydrogen content. Reductions in weld metal hydrogen of almost 70% were achieved with the addition of up to 16.3% micaceous iron oxide. This can be attributed to the formation of oxygen, which lowers the partial pressure of hydrogen in the arc atmosphere, and the reaction of FeO (formed on dissociation of micaceous iron oxide) with hydrogen.
- Additions of silica (SiO_2) to the reference flux formulation brought about a slight decrease in the weld metal hydrogen content. Although SiO_2 additions lower the flux basicity, the observed reduction in weld metal hydrogen content can probably be attributed to a reaction between the SiO_2 and the CaF_2 in the flux formulation. This reactions yields CaO and SiF_4 as reaction products. SiF_4 functions as a shielding gas and reduces the hydrogen partial pressure in the arc, while CaO increases the flux basicity and probably compensates to some extent for the presence of SiO_2 in the slag.
- The addition of fluorine-containing compounds (CaF_2, NaF, K_2TiF_6 or K_2AlF_6) to the reference flux formulation initially resulted in a reduction in the diffusible weld metal hydrogen content. The addition of 22% fluorspar to the flux lowered the average weld metal hydrogen content by about 30%, while the addition of about 8.9% sodium fluoride resulted in a reduction of approximately 40%. The measured weld metal hydrogen contents on addition of K_2TiF_6 and K_2AlF_6 followed a similar

trend. Higher concentrations of these fluorine-containing compounds in the flux seemed to result in an increase in the diffusible weld metal hydrogen content.

- Additions of up to 18% calcite ($CaCO_3$) to the reference flux formulation gave rise to a reduction in the weld metal hydrogen content, but this trend appeared to reverse at higher levels of calcite in the flux coating. The beneficial influence of up to 18% calcite in the flux formulation can be attributed to the formation of CaO, CO and CO_2 as products of the dissociation reaction of $CaCO_3$ in the arc. CaO increases the basicity of the slag, while the presence of CO and CO_2 in the arc atmosphere reduces the partial pressure of hydrogen.

The results of this investigation revealed that the diffusible weld metal hydrogen content decreased to a minimum with the addition of increasing amounts of $CaCO_3$ and fluorine-containing ingredients to the flux formulation. Higher levels of these ingredients in the flux caused an increase in the weld metal hydrogen content. This behaviour can be ascribed to a number of complex reactions, dominated by the amphoteric behaviour of water vapour in the slag and the relationship between the hydroxyl ion capacity and the oxide activity of the slag.

In order to describe the trends observed during this project, the slag water capacity was calculated for a number of slag chemistries determined for experimental flux formulations containing varying amounts of $CaCO_3$ and CaF_2. These calculations showed that the slag water capacity is a strong function, not only of the slag basicity, but also of the slag fluorine content. At a constant basicity, an increase in slag fluorine content, brought about by higher levels of CaF_2 in the flux formulation, decreases the slag water capacity and may result in higher weld metal hydrogen contents. The predicted decrease in slag water capacity with higher levels of fluorine in the slag may therefore account for the higher weld metal hydrogen contents observed on addition of high concentrations of fluorine-containing compounds to the flux.

The results of this investigation therefore confirm that arc chemistry modifications brought about by changes in the electrode flux composition can influence the diffusible weld metal hydrogen content of ferritic steel welds to a significant extent.

A review of the effects of changes in the amounts of various individual raw material ingredients in the flux on the as-deposited weld metal hydrogen content suggests optimal levels of these raw materials with the aim of minimizing the weld metal hydrogen content. These optimal levels are:

- 18% micaceous iron oxide,
- 17.4% fluorspar (CaF_2),
- 4.3% sodium fluoride (NaF), and
- 18% calcite ($CaCO_3$).

As a future project, it is recommended that the combined effect of these additions on the as-deposited weld metal hydrogen content, the weld mechanical properties and the operational characteristics of the electrode be determined experimentally. The results of such an investigation can then be used to optimise the electrode composition in order to ensure low weld metal hydrogen levels, good operating characteristics and adequate mechanical properties after welding.

CHAPTER 7

REFERENCES

[1] Wildash, C., Cochrane, R.C., Gee, R., and Widgery, D.J. *Microstructural factors affecting hydrogen induced cold cracking in high strength steel weldments*. Proceedings of the 5th International Conference on Trends in Welding Research. Pine Mountain. 1-5 June 1998. pp. 745-750.

[2] Davidson, J.L. *Advances in hydrogen management: The science-based design of low hydrogen consumables for the future*. Australian Welding journal, vol. 43. 1998. pp. 33-39.

[3] Pitrun, M., Nolan, D., and Dunne, D. *Correlation of welding parameters and diffusible hydrogen content in rutile flux–cored arc welds.* Australasian Welding Journal, vol. 49. 2004. pp. 33–45.

[4] Matsushita, M., and Liu, S. *Hydrogen control in steel weld metal by means of fluoride additions in welding flux.* Welding Journal, vol. 79, no. 10. October 2000. pp. 295s–303s.

[5] Fleming, D.A., Bracarense, A.Q., Liu, S., and Olson, D.L. *Toward developing a SMA welding electrode for HSLA–100 grade steel.* Welding Journal, vol. 75, no. 6. June 1996. pp. 171s–183s.

[6] Liu, S., Olson, D.L., and Ibarra, S. *Electrode formulation to reduce weld metal hydrogen and porosity.* Proceedings of the 13th International Conference on Offshore Mechanics and Arctic Engineering, vol. 3. Houston. 27 February–3 March 1994. pp. 291–298.

[7] Pokhodnya, I.K., Patsevich, A.P., Golovko, V.V., and Koteltchouk, A.S. *Technology and metallurgy methods for decreasing diffusible hydrogen content.* Welding in the World, vol. 3, no. 4. 1999. pp. 81-90.

[8] AWS Welding Handbook, vol. 2, *Welding Processes – Part I*, 8th edition. AWS, Miami. 1996. p. 44.

[9] Bailey, N., Coe, F.R., Gooch, T.G., Hart, P.H.M., Jenkins, N., and Pargeter, R.J. *Welding Steels without Hydrogen Cracking*, 2nd Edition (revised). Abington Publishing, Cambridge. 2004.

[10] Boellinghaus, T., Hoffmeister, H., and Dangeleit, A. *A scatterband for hydrogen diffusion coefficients in micro–alloyed and low carbon structural steels*. Welding in the World, vol. 35, no. 2. 1995. pp. 83-86.

[11] McKeown, D. *Hydrogen and its control in weld metal.* Metal Construction, vol. 17, no. 10. October 1985. pp. 655-661.

[12] Hirai, Y., Miakawa, S., and Tsuboi, J. *Predictions of diffusible hydrogen content in deposited weld metals and basic type covered electrodes*. IIW Doc II-929-80. 1980.

[13] Grong, ∅,Olson, D.L.,and Christensen, N. *Carnon oxidation in hyperbaric MMA welding.* Metal Construction December 1985. pp.810R -814R.

[14] Chew, B. *Hydrogen control of basic coated MMA welding electrodes – the relationship between coating moisture and weld hydrogen.* Metal construction, vol. 14, no. 7. July 1982. pp. 373-377.

[15] J.F. Lancaster. *Metallurgy of Welding*, 5th Edition. Chapman & Hall, London. 1993.

[16] Olson, D.L., and Liu, S. *The physical and chemical behaviour of steel welding consumables.* Proceedings of the 4th International Conference on Trends in Welding Research. Gatlinburg. 5-8 June 1996. pp. 299-307.

[17] Pargeter, R. *Evaluation of necessary delay before inspection for hydrogen cracks.* Welding Journal, vol. 82, no. 11. November 2003. pp. 321s–329s.

[18] Gedeon, S.A., and Eager, T.W. *Thermochemical analysis of hydrogen absorption in welding.* Welding Journal, vol. 69, no. 7. 1991. pp. 264s–271s.

[19] Gedeon, S.A. *Hydrogen assisted cracking of high strength steel welds*. PhD Thesis, MIT. June 1987.

[20] Palmer, T.A., and DebRoy, T. *Physical modeling of nitrogen partition between the weld metal and its plasma environment.* Welding Journal, vol. 75, no. 7. July 1996. pp. 197s-207s.

[21] Mundra, K., and DebRoy, T. *A general model for partitioning of gases between a metal and its plasma environment.* Metallurgical and Materials Transactions B, vol. 26B. February 1995. pp. 149-157.

[22] Kuwana, T., and Kokawa, H. *The nitrogen absorption of iron weld metal during gas tungsten arc welding.* Transactions of the Japan Welding Society, vol. 17, no. 1. April 1986. pp. 20-26.

[23] Block-Bolten, A., and Eagar, T.W. *Selective evaporation of metals from weld pools.* Proceedings of Trends in Welding Research in the United States. New Orleans. 16-18 November 1981. ASM International, Metals Park. 1982. pp. 53–73.

[24] Hooijmans, J.W., and Den Ouden, G. *A Model of hydrogen absorption during GTA Welding.* Welding Journal, vol. 76, no. 7. July 1997. pp. 264s–268s.

[25] Odengard, O., Evans, G.M., and Christensen, N. *Apparent diffusivity of hydrogen in multi-run weld arc deposits.* Metal Construction, vol. 3, no. 2. 1971. pp. 47-49.

[26] Ban-Ya, S., Hino, M., and Nagasaka, T. *Estimation of water vapour solubility in molten silicates by quadratic formalism based on the regular solution model*. ISIJ International, vol. 33, no. 1. 1993. pp. 12–19.

[27] Chattopadhyay, S., and Mitchell, A. *Thermochemistry of calcium oxide and calcium hydroxide in fluoride slags*. Metallurgical and Materials Transactions B, vol. 21B. August 1990. pp. 621-627.

[28] Rowe, M.D., Liu, S., and Reynolds, T.J. *The effect of ferro–alloy additions and depth on the quality of underwater wet welds*. Welding Journal, vol. 81, no. 8. August 2002. pp. 156s-166s.

[29] Baune, E., Bonnet, C., and Liu, S. *Reconsidering the basicity of a FCAW consumable – Part 2: Verification of the flux/slag analysis methodology for weld metal oxygen control.* Welding Journal, vol. 79, no. 3. March 2000. pp. 66s–71s.

[30] Tuliani, S.S., Boiszewski, T., and Eaton, N.F. *Notch toughness of commercial submerged arc weld metal.* Welding and Metal Fabrication, vol. 8. 1969. pp. 327-339.

[31] Datta, I., and Parekh, M. *Filler metal flux basicity determination using the optical basicity index.* Welding Journal, vol. 68, no. 2. February 1989. pp. 68s–74s.

[32] Terashima, H., and Tsuboi, J. *Hydrogen in submerged arc weld metal produced with agglomerated flux.* Welding Journal of Japan, vol. 45. 1976. pp. 28-33.

[33] Chew B. *Prediction of weld metal hydrogen levels obtained under test conditions*. Welding Journal, vol. 52, no. 9. September 1973. pp. 386s–391s.

[34] Sommerville, I.D., and Yang, Y. *Basicity of metallurgical slags*. AusIMM Proceedings, vol. 306, no. 1. July 2001. pp. 71–77.

[35] Kuzmenko, V.G., and Guzej, V.I. *Pore formation in weld metal in submerged arc welding with surface saturation of grains with fluorine.* The Paton Welding Journal, vol. 2. 2005. pp. 14–17.

[36] Chai, C.S., and Eagar, T.W. *Slag metal reactions in binary CaF_2–metal oxide welding fluxes.* Welding Journal, vol. 61, no. 7. July 1982. pp. 229s–232s.

[37] Nolan, D., and Pitrun, M. *A comparative study of diffusible hydrogen test methods.* Australasian Welding Journal, vol. 48. 2003. pp. 36–41.

[38] Pope, A.M., and Liu, S. *Hydrogen content of underwater wet welds deposited by rutile and oxidizing electrodes*. Proceedings of the 15th International Conference on Offshore Mechanics and Arctic Engineering, Vol. 3 - Materials Engineering. 1996. pp. 85-92.

[39] De Medeiros, R.C., and Liu, S. *A predictive electrochemical model for weld metal hydrogen pick-up in underwater wet welds.* Journal of Offshore Mechanics and Arctic Engineering, vol. 120, no. 248. 1998.

[40] Gaskell, D.R. *Introduction to metallurgical thermodynamics*. McGraw-Hill, 2nd edition. 1981. p. 287.

[41] Grong, Ø., Siewert, T.A., Martins, G.P., and Olson, D.L. *A model for the silicon-manganese deoxidation of steel weld metals*. Metallurgical

and Materials Transactions, vol. 17A, no. 10. October 1986. pp. 1797-1807.

[42] DeVries, R.C., Roy, R., and Osborn, E.F. *Phase equilibria in the system CaO-TiO_2.* Journal of Physical Chemistry, vol. 58. 1954. pp. 1069-1073.

[43] *Slag Atlas*, 2nd edition. Edited by the Verein Deutsche Eisenhüttenleute (VDEh). Verlag Stahleisen GmbH, Düsseldorf. 1995. p. 11.